Inverted direct allorecognition triggers early donor-specific antibody responses after transplantation

Xavier Charmetant, Chien-Chia Chen, Sarah Hamada, David Goncalves, Carole Saison, Maud Rabeyrin, Marion Rabant, Jean-Paul Duong van Huyen, Alice Koenig, Virginie Mathias, et al.

TRANSPLANTATION

Inverted direct allorecognition triggers early donor-specific antibody responses after transplantation

Xavier Charmetant[1]†, Chien-Chia Chen[2]†, Sarah Hamada[3], David Goncalves[1], Carole Saison[3], Maud Rabeyrin[4], Marion Rabant[5], Jean-Paul Duong van Huyen[5], Alice Koenig[1,6,7], Virginie Mathias[3], Thomas Barba[1], Florence Lacaille[8], Jérôme le Pavec[9], Olivier Brugière[10], Jean-Luc Taupin[11,12], Lara Chalabreysse[4], Jean-François Mornex[13,14], Lionel Couzi[15], Stéphanie Graff-Dubois[16], Raphaël Jeger-Madiot[16], Alexy Tran-Dinh[17], Pierre Mordant[18], Helena Paidassi[1], Thierry Defrance[1], Emmanuel Morelon[1,6,7], Lionel Badet[6,19], Antonino Nicoletti[17], Valérie Dubois[3], Olivier Thaunat[1,6,7]*

The generation of antibodies against donor-specific major histocompatibility complex (MHC) antigens, a type of donor-specific antibodies (DSAs), after transplantation requires that recipient's allospecific B cells receive help from T cells. The current dogma holds that this help is exclusively provided by the recipient's CD4$^+$ T cells that recognize complexes of recipient's MHC II molecules and peptides derived from donor-specific MHC alloantigens, a process called indirect allorecognition. Here, we demonstrated that, after allogeneic heart transplantation, CD3ε knockout recipient mice lacking T cells generate a rapid, transient wave of switched alloantibodies, predominantly directed against MHC I molecules. This is due to the presence of donor CD4$^+$ T cells within the graft that recognize intact recipient's MHC II molecules expressed by B cell receptor–activated allospecific B cells. Indirect evidence suggests that this inverted direct pathway is also operant in patients after transplantation. Resident memory donor CD4$^+$ T cells were observed in perfusion liquids of human renal and lung grafts and acquired B cell helper functions upon in vitro stimulation. Furthermore, T follicular helper cells, specialized in helping B cells, were abundant in mucosa-associated lymphoid tissue of lung and intestinal grafts. In the latter, more graft-derived passenger T cells correlated with the detection of donor T cells in recipient's circulation; this, in turn, was associated with an early transient anti–MHC I DSA response and worse transplantation outcomes. We conclude that this inverted direct allorecognition is a possible explanation for the early transient anti-MHC DSA responses frequently observed after lung or intestinal transplantations.

INTRODUCTION

The best therapeutic option for patients with end-stage vital organ failure is organ transplantation, which restores essential physiologic functions through the surgical substitution of the defective organ by a functioning graft retrieved from a donor. However, the antigenic determinants that differ between the donor and the recipient (alloantigens), particularly the highly polymorphic molecules from major histocompatibility complex (MHC) molecules [or human leukocyte antigens (HLA) in human], are inevitably targeted by the adaptive immune system of the recipient. This leads to the failure of the transplanted organ, a process named rejection, which still currently represents the first cause of graft failure (*1*, *2*). Depending on the nature of the adaptive immune effectors responsible for graft destruction, a distinction is made between (i) T cell–mediated rejection (TCMR), in which recipient's T cells infiltrate graft interstitium and destroy the epithelial cells, and (ii) antibody-mediated rejection (AMR) that results from the binding of donor-specific antibodies (DSAs) sequestrated in recipient's circulation to directly accessible donor-specific MHC molecules expressed on graft vasculature (*3*, *4*).

This dichotomic vision of the immunopathology of rejection has long been thought to be the consequence of a unique feature of transplantation: antigen-presenting cells (APCs) can have two origins, donor or recipient, leading to two distinct pathways for allorecognition, direct and indirect (*5*–*7*). Direct allorecognition of donor-specific MHC molecules expressed as intact complexes on the surface of passenger APCs activates up to 10% of a recipient's T cells (*8*), which triggers TCMR. Disappearance of donor bone marrow–derived passenger

[1]CIRI, Centre International de Recherche en Infectiologie, Université de Lyon, INSERM U1111, Université Claude Bernard Lyon 1, CNRS, UMR5308, ENS de Lyon, 69007 Lyon, France. [2]Department of Surgery, National Taiwan University Hospital, Taipei 100, Taiwan. [3]French National Blood Service (EFS), HLA Laboratory, 69150 Décines, France. [4]Department of Pathology, Hospices Civils de Lyon, Groupement Hospitalier Est, 69500 Bron, France. [5]Pathology Department, Assistance Publique-Hôpitaux de Paris, Hôpital Necker, 75015 Paris, France. [6]Lyon-Est Medical Faculty, Claude Bernard University (Lyon 1), 69008 Lyon, France. [7]Department of Transplantation, Nephrology and Clinical Immunology, Hospices Civils de Lyon, Edouard Herriot Hospital, 69003 Lyon, France. [8]Pediatric Gastroenterology-Hepatology-Nutrition Unit, Hôpital Universitaire Necker-Enfants malades, 75015 Paris, France. [9]Department of Pulmonology and Lung Transplantation, Marie Lannelongue Hospital, 92350 Le Plessis Robinson, France. [10]Pulmonology Department, Adult Cystic Fibrosis Centre and Lung Transplantation Department, Foch Hospital, 92150 Suresnes, France. [11]Laboratory of Immunology and Histocompatibility, Hôpital Saint-Louis APHP, 75010 Paris, France. [12]INSERM U976 Institut de Recherche Saint-Louis, Université Paris Diderot, 75010 Paris, France. [13]Université de Lyon, Université Lyon 1, INRAE, IVPC, UMR754, 69000 Lyon, France. [14]Department of Pneumology, GHE, Hospices Civils de Lyon, 69000 Lyon, France. [15]Department of Nephrology, Transplantation, Dialysis, Apheresis, Pellegrin Hospital, 33000 Bordeaux, France. [16]Sorbonne Université, INSERM, Immunology-Immunopathology-Immunotherapy (i3), 75013 Paris, France. [17]Université de Paris, LVTS, INSERM U1148, 75018 Paris, France. [18]Department of Vascular and Thoracic Surgery, Assistance Publique-Hôpitaux de Paris, Bichat-Claude Bernard Hospital, 75018 Paris, France. [19]Department of Urology and Transplantation Surgery, Hospices Civils de Lyon, Edouard Herriot Hospital, 69003 Lyon, France.
*Corresponding author. Email: olivier.thaunat@inserm.fr
†These authors equally contributed to this work.

APCs, which cannot be replenished, provides the explanation to the decay of TCMR incidence reported with time after transplantation (*9*). In contrast, the indirect recognition of allogeneic peptides processed from donor-specific MHC molecules by recipient's APCs and presented within MHC II molecules on their surface activates a smaller number of $CD4^+$ T cells; however, these cells are critically important for the differentiation of allospecific B cells into DSA-producing plasma cells (*10*–*13*). Persistence of indirect response would explain why AMR is the major threat to long-term transplant survival (*1*, *14*–*21*).

Although this dogma provides a general frame compatible with most of the rejection episodes observed in transplant recipients, it fails to explain why some transplant recipients develop episodes of TCMR several years after transplantation (*22*–*24*), at a time when the last donor-derived APC has been eliminated and the direct pathway of allorecognition should be inoperant. This discrepancy led to the discovery in the early 2000s of the semidirect pathway of allorecognition (*25*), by which a recipient's cytotoxic T cells of "direct specificity" can recognize intact allogeneic MHC molecules displayed on recipient APCs (MHC cross-dressing) after their transfer through cell-cell contact (*26*) or through extracellular vesicles (*27*, *28*). Persistence of this pathway for the life of the transplant explains the sustained activation of direct-pathway T cells and the occurrence of late TCMR episodes (*29*, *30*). Recent reevaluations of the respective contribution of direct and semidirect pathways suggest that it is the latter that is the dominant mechanism triggering TCMR, including immediately after transplantation (*27*, *31*).

Inspired by the progress made in the understanding of TCMR pathophysiology and by another recent study (*32*), we initiated this translational study aiming at reassessing the importance of the indirect pathway in the pathophysiological sequence leading to AMR. Combining murine experimental models with the analysis of renal, lung, and intestine recipients, we confirmed that $CD4^+$ T cell help is indeed mandatory for DSA generation. However, when the grafted organ contains a high number of donor $CD4^+$ T cells (which is the case for graft containing professional secondary lymphoid tissue), these passenger $CD4^+$ T cells can interact with recipient's B cells through direct allorecognition of intact recipient's MHC molecule and provide help for DSA generation. This transient, inverted direct pathway is responsible for the early onset of DSA generation, which can have a detrimental impact on graft survival.

RESULTS

CD3ε knockout recipient mice develop alloantibodies after heart transplantation

Current dogma in transplant immunology holds that the generation of alloantibody against donor-specific MHC proteins depends on a prototypical T cell–dependent humoral response. After the binding of donor-specific MHC molecules to their B cell receptor (BCR) that delivers the first signal of activation, recipient allospecific B cells indeed need a second signal of activation that is thought to come from cognate interactions with recipient's $CD4^+$ T cells. This implies that the T cells involved in the alloantibody response are of indirect specificity, meaning that their T cell receptor (TCR) is specific for the complexes consisting of a recipient's MHC and a peptide derived from a donor's MHC molecule.

Aiming at testing the dependency of alloantibody response to recipient's T cells, we used CD3ε knockout (KO) mice. CD3ε is a signaling component of the TCR complex, the genetic ablation of which impedes the positive selection of T cells in the thymus. Thus, CD3εKO mice showed complete elimination of $CD3^+$ T lymphocytes in their spleen, lymph nodes, and peripheral blood mononuclear cells (PBMCs; fig. S1A). Because this genetic manipulation has no impact on B cell ontogeny, CD3εKO mice exhibited a normal $CD19^+$ B cell count (fig. S1A). To further document the lack of T cell help and the functionality of B cell compartment in this strain, CD3εKO mice were immunized with either the thymo-independent or the thymo-dependent forms of the model hapten 4-(hydroxy-3-nitro-phenyl) acetyl (NP) antigen. Whereas CD3εKO and wild-type (WT) C57BL/6 mice developed similar anti-NP immunoglobulin M (IgM) response after immunization with NP-dextran (a known thymo-independent antigen due to its polysaccharide structure), only WT mice developed anti-NP IgG after immunization with the thymo-dependent NP–keyhole limpet hemocyanin (KLH) antigen (fig. S1B).

To specifically address the question of the dependency of the alloantibody response to recipient's T cell help, a fully allogeneic (CBA; $H\text{-}2^k$) heart graft was transplanted heterotopically into WT or CD3εKO C57BL/6 ($H\text{-}2^b$) recipients (Fig. 1A). The donor-specific antibody (DSA) responses against the donor's MHC molecules were assessed by flow cross-match using CBA ($H\text{-}2^k$) $CD4^+$ T cells. As expected, WT recipients developed DSAs, which became detectable from day 14 onward and reached a peak around day 28 (Fig. 1B). However, unexpectedly, T cell–deficient CD3εKO recipients also generated DSAs (Fig. 1B).

The alloantibody response of CD3εKO recipients is early and transient

A custom single-antigen bead assay, similar to the one used in routine clinical practice, was used to compare the specificity and intensity of the DSA response of the two groups of recipient mice. Although CD3εKO recipients generated the same concentration of anti–MHC I alloantibodies as WT controls, the former produced much less DSAs directed against donor-specific MHC II (Fig. 1C). DSAs generated by CD3εKO recipients were, nevertheless, deleterious because they were able to trigger the development of microvascular inflammatory lesions in the heart allograft (Fig. 1D).

Analyzing the kinetics of the alloimmune humoral response more precisely revealed that CD3εKO recipients developed DSAs with faster kinetics as compared with WT recipients ($P = 0.0082$, log-rank test; Fig. 1, B and E) but their DSA titers rapidly decayed after the peak ($P = 0.0123$, log-rank test; Fig. 1, B and F). Because these two features are evocative of a T cell–independent B cell response, which are exclusively made of IgM and IgG3, we next analyzed the heavy chain isotype of the DSAs generated by WT and CD3εKO recipients. At the peak of the antibody response, the DSAs generated by CD3εKO recipients were not predominantly IgM and IgG3 (Fig. 1G). Except a lower amount of IgG1, the profile of the heavy chain isotypes of DSAs generated by CD3εKO recipients was similar to that of WT recipients (Fig. 1G).

Together with the fact that donor MHC molecules are proteins and not sugar antigens, this suggested that DSA response in CD3εKO recipients did not result from a T cell–independent humoral response. This therefore raised the intriguing question of how CD3εKO recipients develop T cell–dependent DSA responses when they have no T cells (fig. S1A) to provide help to their alloreactive B cells.

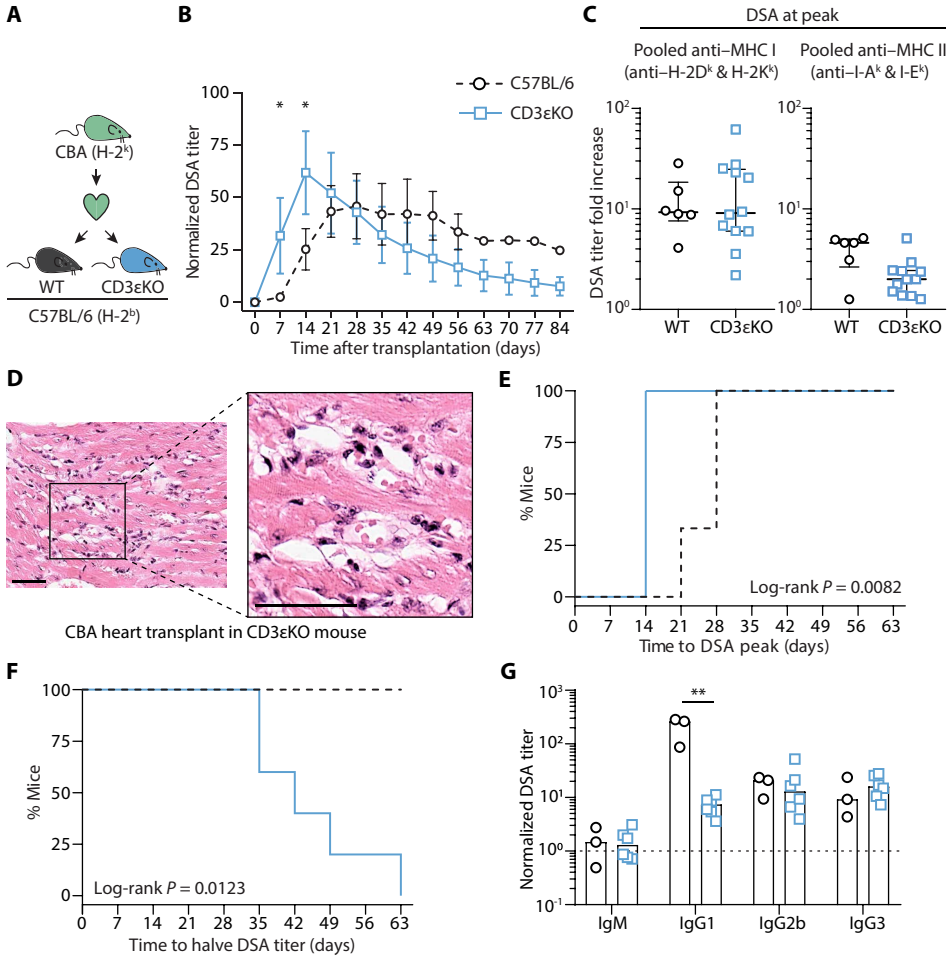

Fig. 1. CD3εKO recipient mice develop alloantibodies after transplantation. (**A**) Presentation of the mouse model. Allogeneic CBA (H-2^k) hearts were transplanted to wild-type (WT) or CD3εKO C57BL/6 (H-2^b) recipient mice. Results are from two independent experiments. (**B**) Development of normalized anti–MHC I DSA titers in the circulation of recipients is shown for WT C57BL/6 ($n = 3$; black circles) and CD3εKO ($n = 6$; blue squares). Data are presented as means ± SD. Data were analyzed by multiple t tests. *$P < 0.05$. (**C**) DSAs were analyzed in WT (black circles) and CD3εKO (blue squares) recipients between day 14 (D14) and D28 after transplantation. Serum samples were screened for the presence of anti–MHC I (left) or anti–MHC II (right) antibodies using a custom single-antigen bead assay. Bars indicate the median and interquartile ranges (IQR). (**D**) Representative histological findings of an allogeneic CBA (H-2^k) heart graft after transplantation to a CD3εKO recipient. Hematoxylin and eosin staining is shown. Scale bars, 50 μm. Kaplan-Meyer curves of (**E**) the delay between transplantation and DSA peak or (**F**) the peak and the time to halve DSA titers for WT ($n = 3$; dashed black line) and CD3εKO ($n = 6$; blue line) recipients. (**G**) Anti-MHC DSA isotypes were tested at the peak of the response. Individual values (and median value) of normalized titers are represented. The horizontal dashed line indicates the positivity threshold. Data were analyzed by Mann-Whitney test. **$P < 0.01$.

DSAs can be generated with the help of CD4$^+$ T cells from the donor

To further examine the role of CD4$^+$ T cells in the generation of DSAs in CD3εKO recipients, we conducted a series of experiments, in which the recipients were treated with depleting anti-CD3 (clone 17A2) or anti-CD4 (clone GK1.5) monoclonal antibodies (mAbs). Treatment with both depleting mAbs drastically reduced DSA response of CD3εKO recipients (Fig. 2A). This result demonstrates that the interaction of CD4$^+$ T cells with B cells is essential to generate DSA, including in CD3εKO recipients.

Because CD3εKO recipients completely lack T cells (fig. S1A) and fail to mount T cell–dependent humoral response upon immunization with a model protein antigen (fig. S1B), we hypothesized that the CD4$^+$ T cells providing help to recipient's alloreactive B cells could originate from the graft. In support of this theory, around 4500 CD4$^+$ T cells were observed in the cell suspensions obtained after collagenase digestion of heart grafts (Fig. 2, B and C). To further demonstrate the role of these passenger CD4$^+$ T cells in the DSA response of CD3εKO recipients, anti–CD3- or anti–CD4-depleting mAbs were administered to the donor animals before harvesting of the heart. CD4$^+$ T cells were efficiently depleted with both mAbs, both in the heart and the periphery of donor mice, albeit with slightly different kinetics (Fig. 2C). Heart grafts were collected at the nadir of CD4$^+$ T cell count (day 1 after anti-CD3 injection and day 7 after anti-CD4 injection; Fig. 2C) and transplanted into CD3εKO recipients. CD3$^+$ or CD4$^+$ T cell depletion in the donor not only abrogated DSA response in recipients (Fig. 2D) but also drastically reduced microvascular inflammatory lesions within the graft (Fig. 2E), thus suggesting that donor's CD4$^+$ T cells present within the graft are able to provide the help required by recipient's alloreactive B cells to differentiate into DSA-producing plasma cells.

The existence of this allorecognition pathway, distinct from the canonical indirect pathway but capable of triggering the generation of deleterious DSAs, was later confirmed by the demonstration that the mere transfer of allogeneic CBA (H-2^k) CD4$^+$ T cells was sufficient to trigger the generation of DSAs in C57B/L6 (H-2^b) CD3εKO mice (Fig. 2F). Furthermore, using this simplified model, we highlighted that this allorecognition pathway was critically dependent on the number of allogeneic CD4$^+$ T cells injected in the circulation of the recipient (Fig. 2G). Furthermore, because no DSA was generated (even with the higher number of allogeneic CD4$^+$ T cells) when cells were fixed before the transfer (Fig. 2G), we concluded that this allorecognition pathway requires that the allogeneic CD4$^+$ T cells are functional.

Donor's CD4$^+$ T cells recognize allogeneic MHC II on the surface of the recipient's B cells

The sequence leading to the generation of DSA through the canonical indirect pathway is well known (Fig. 3A). The recognition of donor-specific MHC molecules by the BCR delivers the first signal of activation to recipient allospecific B cells and induces the internalization of the alloantigen. To complete their differentiation, allospecific B cells need to present alloantigen-derived peptides within surface MHC II molecules. Only when these complexes are recognized by

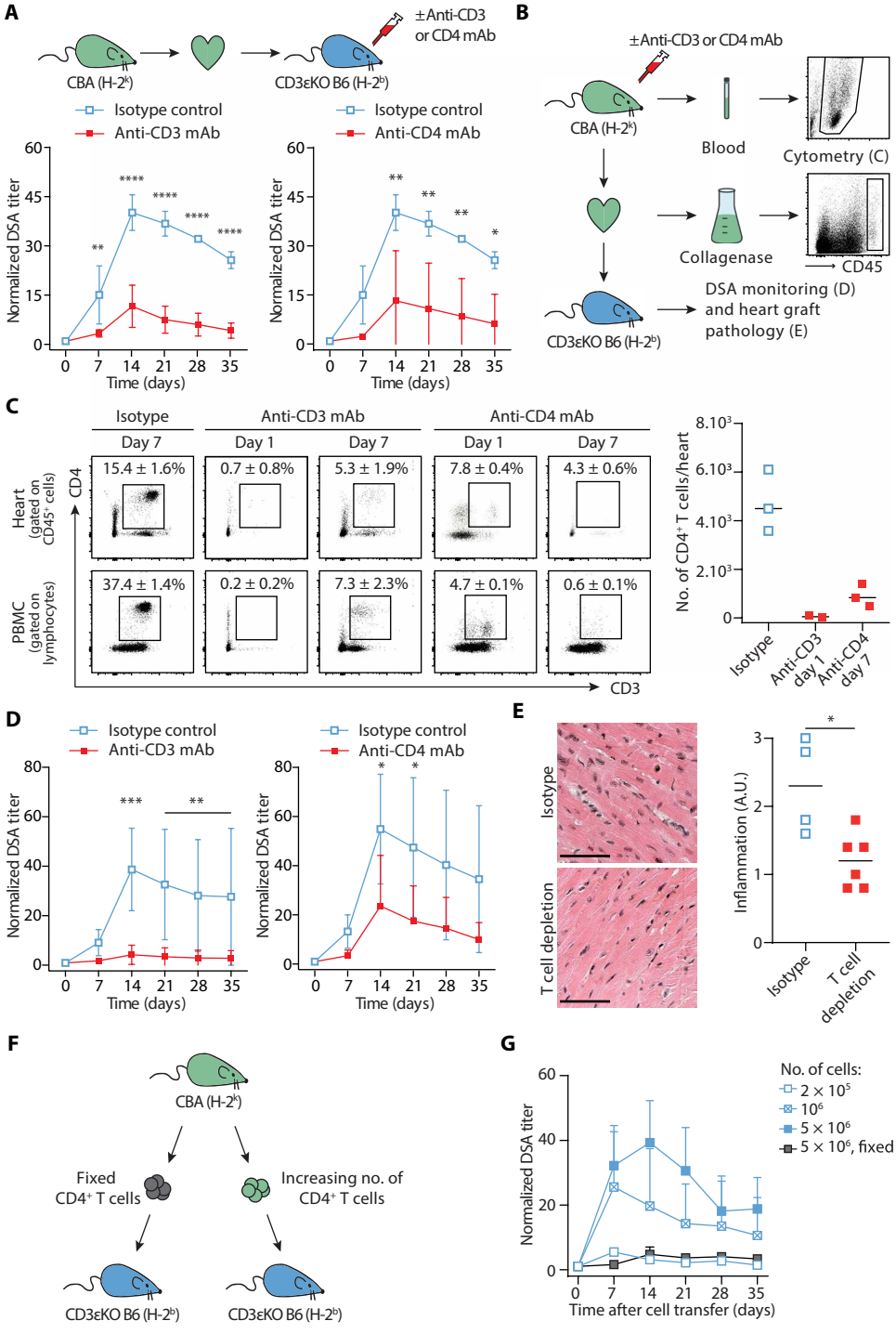

Fig. 2. DSA generation requires CD4$^+$ T cells, which can originate from the donor. (**A** to **E**) Allogeneic CBA (H-2^k) hearts were transplanted to CD3εKO C57BL/6 (H-2^b) recipient mice. (A) Recipient mice were injected intravenously after transplantation with either a depleting anti-CD3 mAb (left; red curve; $n = 4$), a depleting anti-CD4 mAb (right; red curve; $n = 4$), or an isotype control (blue curve). Evolution of normalized anti-MHC DSA titers is shown (means ± SD). Data were analyzed by multiple *t* tests. *$P < 0.05$, **$P < 0.01$, and ****$P < 0.0001$. (B) Donor CBA mice were injected intravenously with either a depleting anti-CD3 mAb, a depleting anti-CD4 mAb, or an isotype control before flow cytometry analysis or heart transplantation. (C) Heart grafts were harvested 1 or 7 days after mAb injection and digested with collagenase. Heart graft cell suspension (top rows) and PBMCs (bottom rows) were analyzed by flow cytometry. Representative flow cytometry profiles. The far-right plot shows the absolute number of CD4$^+$ T cells isolated from murine heart grafts from the three groups. Horizontal bars indicate the median. (D) Evolution of normalized anti-MHC DSA titers (means ± SD) was measured in CD3εKO recipients of a CBA heart harvested either after anti-CD3 treatment (top row; red curve; $n = 4$), anti-CD4 treatment (bottom row; red curve; $n = 4$), or isotype control treatment (blue curve; $n = 3$). Data were analyzed by multiple *t* tests. *$P < 0.05$, **$P < 0.01$, and ***$P < 0.001$. (E) CBA (H-2^k) heart grafts harvested from mice previously injected intravenously with either an isotype control ($n = 4$; top image, blue) or a T cell–depleting mAb ($n = 6$; bottom image, red) were transplanted into CD3εKO C57BL/6 (H-2^b) recipients. Left: Representative hematoxylin and eosin staining. Scale bars, 50 μm. Right: The intensity of microvascular inflammatory lesions, which was graded on a semiquantitative scale (score 0 to 3). Horizontal bars indicate the median. Data were analyzed by Mann-Whitney test. *$P < 0.05$. A.U., arbitrary units. (**F** and **G**) Purified allogeneic CBA (H-2^k) CD4$^+$ T cells were injected intravenously to CD3εKO (H-2^b) recipient mice. Evolution of normalized anti-MHC DSA titers was measured (means ± SD). (F) Schematic representation of the experiments. (G) Indicated numbers of alive (blue curves) or alcohol-fixed (black curve) purified allogeneic CBA CD4$^+$ T cells (2×10^5 to 5×10^6) were injected intravenously to WT C57BL/6 (H-2^b) recipient mice, and DSA titers were analyzed at the indicated times after cell transfer.

the recipient's cognate CD4$^+$ T cells can the latter deliver the "second" signal of activation to allospecific B cells.

To test whether MHC II expression on recipient's B cells was also important for their interaction with donor's CD4$^+$ T cells, we transferred purified allogeneic (CBA; H-2^k) CD4$^+$ T cells to C57B/L6 (H-2^b) recombination activating gene 2 (Rag2) KO recipient mice that had been previously replenished by adoptive transfer of syngeneic B cells purified from either WT (controls) or MHC class II I-A β chain KO (referred to as "AβKO") C57B/L6 mice. As the result of the genetic ablation of the I-A β chain, none of the cells of AβKO mice, including B cells, expresses MHC II molecules. This lack of MHC II expression in the thymus also disrupts positive selection of CD4$^+$ T cells, which are totally absent from the PBMCs, the spleen, and the lymph nodes of these animals (fig. S1A). As expected, AβKO mice can therefore neither generate antibody after immunization with the T cell–dependent antigen NP-KLH (fig. S1B) nor generate DSA through

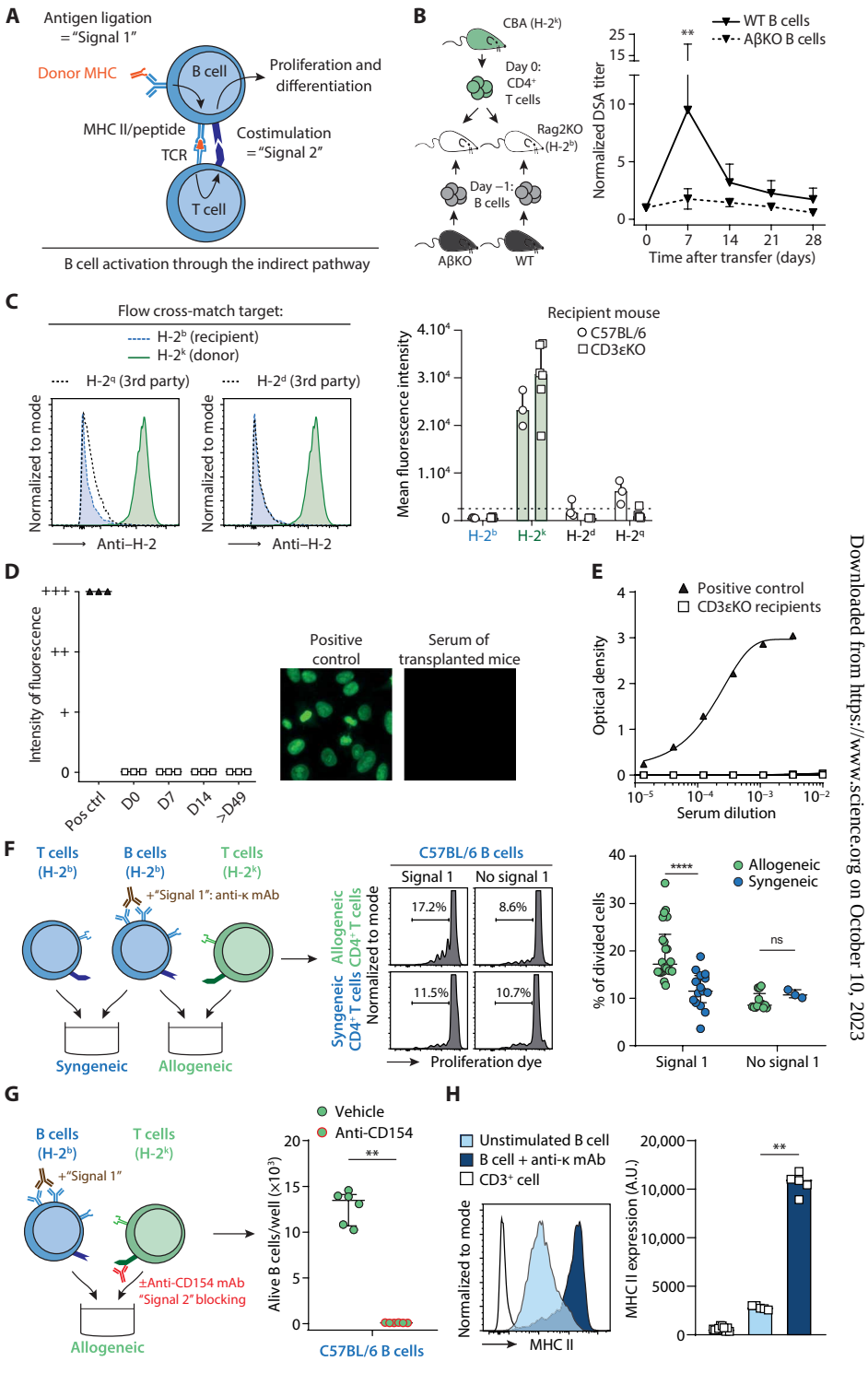

Fig. 3. Donor CD4$^+$ T cells recognize allogeneic MHC II on the surface of antigen-activated recipient allospecific B cells. (**A**) Schematic representation of the molecular requirements for B cell activation through the canonical indirect pathway. (**B**) Purified allogeneic CBA (H-2^k) CD4$^+$ T cells were injected intravenously to Rag2KO C57BL/6 (H-2^b) mice. The day before the T cell transfer, 5×10^6 B cells were purified from WT (black curve; $n = 6$) or AβKO (dashed black curve; $n = 4$) mice (H-2^b) and were injected intravenously to Rag2KO mice. Data were analyzed by multiple *t* tests. Data are presented as means ± SD. $^{**}P < 0.01$. (**C**) Serum samples from WT and CD3εKO recipients were collected at the peak of the DSA response and incubated with different cells expressing recipient (H-2^b), donor (H-2^k), or third-party (H-2^q or H-2^d) MHC molecules. Left: Representative histograms. Right: Mean fluorescence intensity values. Data are presented as median ± IQR. The horizontal dashed line indicates negative controls. (**D**) Serum from CD3εKO mice transplanted with allogeneic CBA hearts ($n = 3$) were screened for the presence of autoantibodies by indirect immunofluorescence on Hep-2 cells; representative images are shown on the right. Individual semiquantitative evaluations are shown. Serum from three mice with lupus was used as positive controls. (**E**) Serum from CD3εKO mice transplanted with allogeneic CBA hearts ($n = 6$) was screened for the presence of anti-NP antibodies by enzyme-linked immunosorbent assay. Curves representing the optical density as a function of the sample's concentration are shown. Serum from one WT mouse immunized with NP-KLH was used as a positive control. (**F**) C57BL/6 (H-2^b) B cells, activated or not by BCR cross-linking with anti-κ mAb (signal 1), were cocultured with syngeneic or allogeneic (CBA; H-2^k) CD4$^+$ T cells. Left: The schematic representation of the experiments. Middle: Representative flow cytometry histograms. The median percentage of divided B cells is shown. Right: Individual coculture values. Data are presented as median ± IQR. Data were analyzed by Mann-Whitney tests. $^{****}P < 0.0001$. ns, nonsignificant. (**G**) BCR-activated C57BL/6 B cells were cocultured with CBA CD4$^+$ T cells in the presence or absence of blocking anti-CD154 mAb. The number of alive B cells was measured by flow cytometry. Left: A schematic representation of the experimental cocultures. Right: Individual coculture values. Data are presented as median ± IQR. Data were analyzed by Mann-Whitney test. $^{**}P < 0.01$. (**H**) MHC II expression was quantified on the surface of B cells before and after BCR cross-linking with anti-κ mAb. Left: Representative histograms. Right: Individual mean fluorescence intensity values. Bars indicate median values. Data were analyzed by Mann-Whitney test. $^{**}P < 0.01$.

the canonical indirect pathway. However, because the genetic manipulation has no impact on B cell ontogeny, AβKO mice exhibited normal CD19$^+$ B cell count (fig. S1A) and mounted an antibody response after immunization with the T cell–independent antigen NP-dextran (fig. S1B). In contrast with Rag2KO mice replenished with WT B cells, those injected with AβKO B cells did not generate DSA after the transfer of allogeneic CBA (H-2^k) CD4$^+$ T cells (Fig. 3B). Furthermore, the same lack of DSA generation was obtained when AβKO recipients were transplanted with an allogeneic CBA heart (fig. S2). This demonstrates that the expression of MHC II molecules on the surface of the recipient's B cells is mandatory for their interaction with the donor's CD4$^+$ T cells. We therefore called this pathway of allorecognition the "inverted direct pathway" because T cells recognize intact allogeneic MHC molecules on the surface of

the APC, as in canonical direct allorecognition. However, in this case, the origin of the interacting cells is "inverted" as compared with canonical direct allorecognition: T cells come from the donor and recognize intact recipient's MHC class II molecules on allospecific B cells.

The humoral response triggered by the inverted direct pathway is allospecific

Because B cells are professional APCs, they constitutively express MHC II on their surface. This implies that alloreactive donor's $CD4^+$ T cells could theoretically interact with any recipient's B cell, regardless its BCR specificity, and, therefore, that the control of the specificity of the B cell response might be lost in the inverted direct pathway. In disagreement with this hypothesis, however, we did not detect any antibody directed against third-party ($H\text{-}2^d$ and $H\text{-}2^q$) MHC molecules in the serum of CD3εKO recipients ($H\text{-}2^b$) of an allogeneic CBA ($H\text{-}2^k$) heart (Fig. 3C). Screening for autoantibodies (Fig. 3D) or antibodies directed against an irrelevant model antigen (Fig. 3E) was equally negative. The humoral alloimmune response of CD3εKO recipients, in which only the inverted direct pathway is functional, targeted exclusively donor-specific MHC molecules, exactly similar to that of WT controls, except for a quantitative bias toward MHC I (Fig. 1C). These results raise the intriguing question of what molecular mechanisms maintain the alloantigen specificity in the antibody response triggered by this inverted direct pathway.

Inverted direct allorecognition requires BCR and costimulatory signals

To dissect the molecular requirements for the dialog between recipient's B cells and donor's $CD4^+$ T cells and shed light on how this unconventional T cell help manages to maintain the antigen specificity of the antibody response, we moved to in vitro models. To deliver the first (BCR-mediated) signal of activation to purified WT murine B cells in culture, we used an anti-κ light chain mAb. By cross-linking surface BCRs, the latter triggers downstream signaling in a high proportion of polyclonal B cells (fig. S3, A and B) with an intensity similar to that observed when the cognate antigen binds to the BCR of specific B cell clone (fig. S3, A and B). This strategy therefore allowed us to test the importance of the first signal of activation independently of the alloantigen itself and its subsequent presentation within the MHC II molecules of activated B cells.

After 3 days, B cells proliferated more when cocultured with allogeneic than syngeneic $CD4^+$ T cells [17.2%, interquartile range (IQR) 15.7 to 23.5 versus 11.5%, IQR 9.1 to 14.8 divided B cells, $P < 0.0001$; Fig. 3F]. However, this difference was only observed if B cells were previously activated with anti-κ mAb. When the same B cell–T cell cocultures were performed with resting B cells, the amount of divided B cells was low and not different between the two coculture conditions (8.6%, IQR 8.1 to 11.0 versus 10.7%, IQR 10.1 to 11.8 $P = 0.182$; Fig. 3F). In line with the results shown in Fig. 3B and fig. S2A, signal 1–primed B cells from AβKO mice (which do not express MHC II) did not proliferate, regardless of whether they were cocultured with allogeneic or syngeneic $CD4^+$ T cells (fig. S4). Last, we investigated the molecular nature of the second signal of activation delivered by donor T cells to the recipient's B cells. Given the importance of CD154 (also known as CD40L)/CD40 costimulation in canonical B cell responses to T cell–dependent antigens (*33*), we hypothesized that it could also be crucial in this allorecognition pathway. To test this hypothesis, C57BL/6 B cells were primed with anti-κ light chain mAb and were then cocultured with allogeneic CBA $CD4^+$ T cells with or without anti-CD154 blocking mAb. In line with our hypothesis, blocking anti-CD154 mAb in the coculture resulted in the death of activated B cells (Fig. 3G).

We next asked why BCR stimulation was critical for the recipient's B cells to interact with the cognate donor's $CD4^+$ T cells if the antigen is dispensable and MHC II and CD40 are expressed on the surface of unstimulated B cells. It has been shown previously that concurrent engagement of BCR and CD40 provides B cells with a critical advantage and protects them from Fas-mediated apoptosis (*34*, *35*). Furthermore, the cross-linking of surface BCR induced a strong up-regulation of MHC II expression on the surface of B cells (15891, IQR 14678 to 16432 versus 2748, IQR 2630 to 3005 $P = 0.0079$; Fig. 3H), hence increasing the number of molecular targets that can be directly recognized by the TCR of donor T cells of direct specificity. The BCR stimulation that makes B cells fit to interact with donor T cells is not provided by artificial anti-κ mAb in vivo but by alloantigens coming from the graft, the most abundant of which is donor-specific MHC I molecules (which are expressed by all the cells of the graft). We hypothesize that this could be the reason why the antibody response triggered through the inverted direct pathway is restricted to alloantigen and biased toward donor-specific MHC I (Fig. 1C).

Human allogeneic T cells provide help to B cells in vitro

To test whether inverted direct allorecognition pathway could be of clinical importance, we adapted the murine in vitro model described above to human T and B cells. Similar to what was observed in mice, BCR cross-linking with anti-IgM $F(ab')_2$ resulted in up-regulation of MHC II expression by purified human B cells in culture (fig. S5). Furthermore, BCR-mediated stimulation also resulted in up-regulation of several key costimulatory molecules (including CD40, CD80, and CD86) involved in T cell activation (fig. S5). In line with this observation, as in mice, only signal 1–primed human B cells proliferated when cocultured with allogeneic human $CD4^+$ T cells (Fig. 4A).

To further demonstrate that human B cells and allogeneic T cells establish cognate interactions in cocultures, we analyzed trogocytosis, which corresponds to an active transfer of surface molecules between cellular partners closely interacting, such as in the case of immunological synapse formation (*36*). We observed that B cells cocultured with allogeneic T cells captured significantly more CD4 molecules (22.5%, IQR 15.4 to 33.8 versus 9.8%, IQR 6.8 to 13.8 $P = 0.004$; Fig. 4B). Therefore, we concluded that human B cells require the same conditions as murine B cells to proliferate efficiently. These results suggest that the production of early DSA by the inverted direct allorecognition pathway could occur in patients after organ transplantation, provided that donor $CD4^+$ T cells are present in human transplants.

Passenger T cells present within kidney graft acquire costimulation capabilities upon activation

Machine perfusion is a technique used in transplantation to preserve the organs after their removal from the donor (Fig. 4C). Briefly, the grafts are rinsed from the donor's blood before being connected to a machine that generates a controlled recirculating flow of the preservation solution at 4°C. To investigate the presence of donor $CD4^+$ T cells within kidney grafts, we took advantage of this procedure and prospectively collected 37 kidney graft perfusion liquids. The perfusion liquids were collected right at the end of the procedure (median

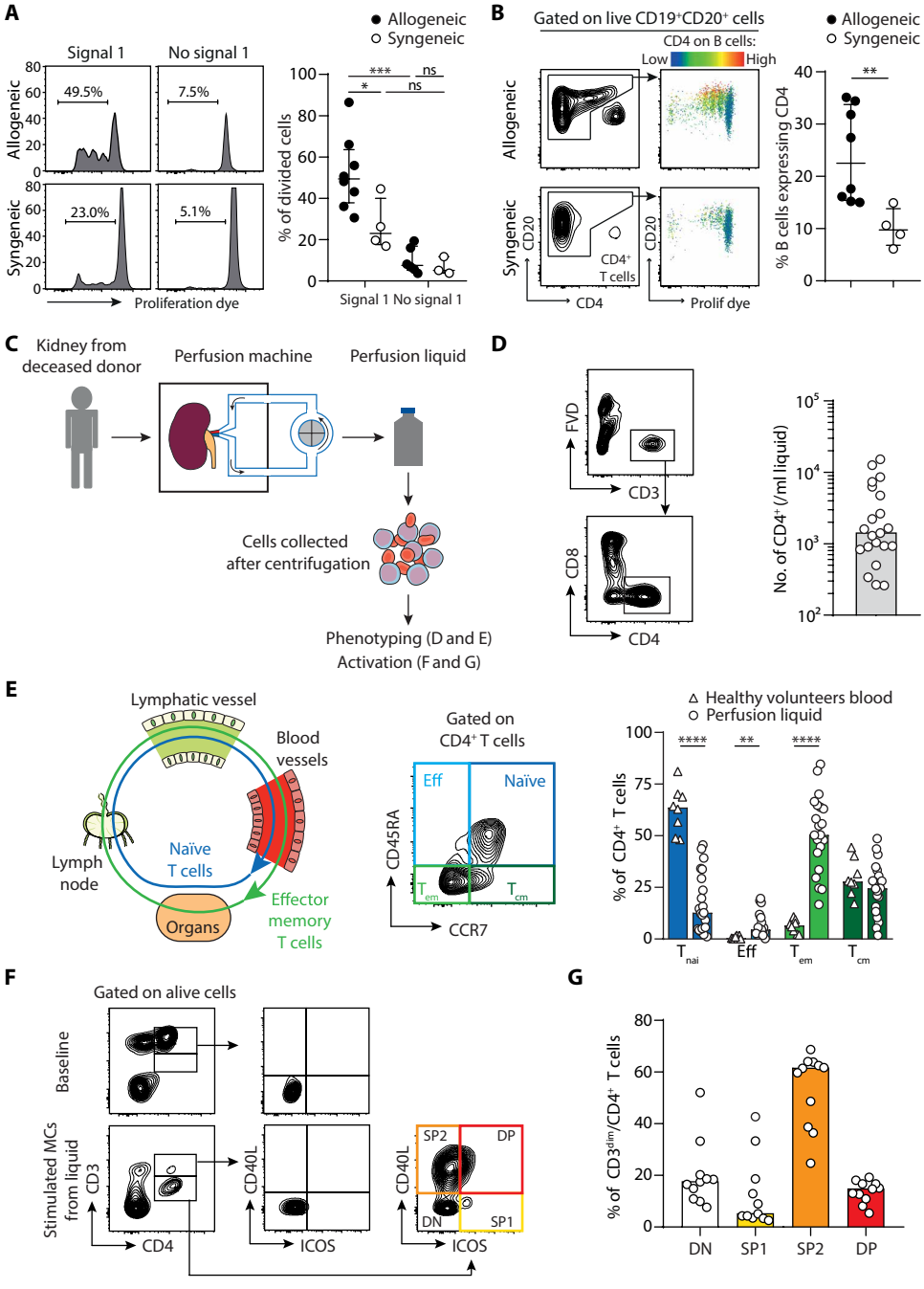

Fig. 4. Human allogeneic T cells present in kidney grafts can provide help to B cells in vitro. (**A**) Human B cells were cocultured with syngeneic or allogeneic CD4$^+$ T cells in the presence or not of IgM F(ab')$_2$ (signal 1), and the percentage of divided cells among alive B cells was evaluated by flow cytometry. Left: Representative histograms with median value for each condition. Right: Individual coculture values. Data are presented as median ± IQR. Data were analyzed by Mann-Whitney test. *P < 0.05 and ***P < 0.001. (**B**) Human B cells activated with IgM F(ab')$_2$ were cocultured with syngeneic or allogeneic CD4$^+$ T cells. Left: The flow cytometry gating strategy for the assessment of trogocytosis. Right: The percentage of B cells that have experienced trogocytosis in each coculture. Data are presented as median ± IQR. Data were analyzed by Mann-Whitney test. **P < 0.01. (**C**) Perfusion fluids of renal allograft were collected (n = 37) at the end of procedure, and the phenotype of the immune cells that passed from the graft to the fluid was determined by flow cytometry. (**D**) Representative flow profiles and the flow cytometry gating strategy are shown for the analysis of renal allograft perfusion fluids (left). The number of CD4$^+$ T cells that contained per milliliter of perfusion fluid was quantified (right). FVD, fixable viability dye. (**E**) Left: A schematic representation of the circulation behavior of the different T cell subsets. Middle: A representative flow profile for T cell phenotyping. Right: The percentages of naïve (T_{nai}), effector (Eff), effector memory (T_{em}), and central memory (T_{cm}) CD4$^+$ T cells found in renal allograft perfusion fluids (open circles) as compared with those observed in the blood of eight healthy volunteers (triangles). Bars indicate median values. Data were analyzed by Mann-Whitney test. **P < 0.01 and ****P < 0.0001. (**F** and **G**) Mononuclear cells (MCs) isolated from renal allograft perfusion fluids were stimulated (or not) with anti-CD3/anti-CD28 nanoparticles. Flow cytometry was used to measure the surface expression of CD40L and ICOS. (F) The flow cytometry gating strategy is shown. SP, single positive; DP, double positive; DN, double negative. (G) The percentages of the various CD4$^+$ T cell subsets observed after activation are plotted for the 11 renal allograft perfusion fluids analyzed. Bars indicate median values.

perfusion length 630 min; range, 245 to 1195) and centrifugated to isolate the cells, which were then analyzed by flow cytometry (Fig. 4D). Kidney grafts did contain passenger mononuclear cells, including CD4$^+$ T cells (Fig. 4D).

Although kidneys are rinsed before being connected to the perfusion machine, contamination with the donor's blood remains possible. To evaluate the importance of this potential bias, we compared the ratios of red and white blood cells in paired blood and perfusion liquid samples. We observed that white blood cells were 34.4-fold more abundant in the perfusion liquid than in the blood. In addition, the distribution between the various CD4$^+$ T subsets in perfusion liquid was different from that observed in the blood of healthy volunteers (Fig. 4E). Perfusion liquids were largely enriched with CCR7$^-$CD45RA$^-$CD4$^+$ effector memory T cells, a subset localized within tissue, and were deprived of circulating CCR7$^+$CD45RA$^+$CD4$^+$ naïve T cells (Fig. 4E). These results suggest that cell populations identified in perfusion liquids reflect the cellular content of human kidney grafts. Although passenger CD4$^+$ T cells did not express the surface molecules typically associated with B helper function at baseline, a strong up-regulation of CD40L expression [and, to a lesser extent, inducible T cell costimulatory (ICOS)] was observed on their surface after TCR stimulation (Fig. 4, F and G).

Early DSA generation depends on the graft content in a donor's T cells in humans

Recipient's B cells are located within secondary lymphoid organs: lymph nodes and spleen. The lymphatic vasculature of the graft is not anastomosed to that of the recipient during the surgical procedure, and reestablishment of the lymphatic outflow takes several days (*37*, *38*). In line with this, it has been shown that after the transplantation of a vascularized organ, donor passenger leukocytes are found in the recipient's spleen (homing through blood) rather than in lymph nodes (homing through lymph) (*39*). We therefore reasoned that passenger $CD4^+$ T cells should be detectable in recipient's circulation immediately after transplantation if they were to reach the spleen and interact with the recipient's B cells to generate a first early wave of DSAs. Chimerism analysis of the circulating $CD3^+$ compartment was performed during the first 3 days after kidney transplantation in nine consecutive recipients. Despite the fact that kidney grafts contain passenger T cells (Fig. 4), T cells of donor origin could only be detected (and at very low abundance) in the circulation of a single patient (Fig. 5A). This is likely explained by the fact that (i) kidney grafts contain relatively few passenger T cells and (ii) 6 of 15 tested kidney recipients received thymoglobulin as induction therapy (but not the one with positive chimerism).

In contrast with the kidney, the lung contains a professional lymphoid tissue [bronchus-associated lymphoid tissue (BALT)]. Computer-assisted morphometric quantification showed that a lung contains on average 11.5-fold more $CD4^+$ T cell per surface unit than a kidney (Fig. 5B). This difference does not take into account the size difference between the two organs (a lung weighs about 420 g versus only about 130 g for a kidney), and most of the time, two lungs are transplanted together to the recipients. In total, we estimated that lung recipients receive about 74-fold more donor T cells than kidney recipients. Together with the fact that depleting induction is rarely used in thoracic transplantation centers, these differences likely explain why all lung recipients tested had high amounts (up to 20%) of $CD3^+$ T cells from donor origin detectable in their circulation the day after transplantation (Fig. 5A). Although a clear trend for diminution was noted afterward, this chimerism persisted for several days (Fig. 5A).

The phenotype of the passenger $CD4^+$ T contained in the perfusion liquids of lung transplants was analyzed by flow cytometry as for kidney grafts (Fig. 5C). Beyond the mere quantitative aspect mentioned above, there was also a difference in the nature of the passenger T cells between the two types of grafts. BALT is a professional secondary lymphoid tissue, which contains T follicular helper cells (T_{FH}), a subset of $CD4^+$ T cells specialized in providing help to B cells (*11*, *12*, *40*). T_{FH} are constitutively equipped with CXCR5, a chemokine receptor that allows T_{FH} to migrate efficiently in B cell areas (*11*, *12*, *40*). As expected, up to 10% of passenger $CD4^+$ T cells were $CXCR5^+$ T_{FH} in lungs, whereas they represented only 5% in the kidneys (Fig. 5D).

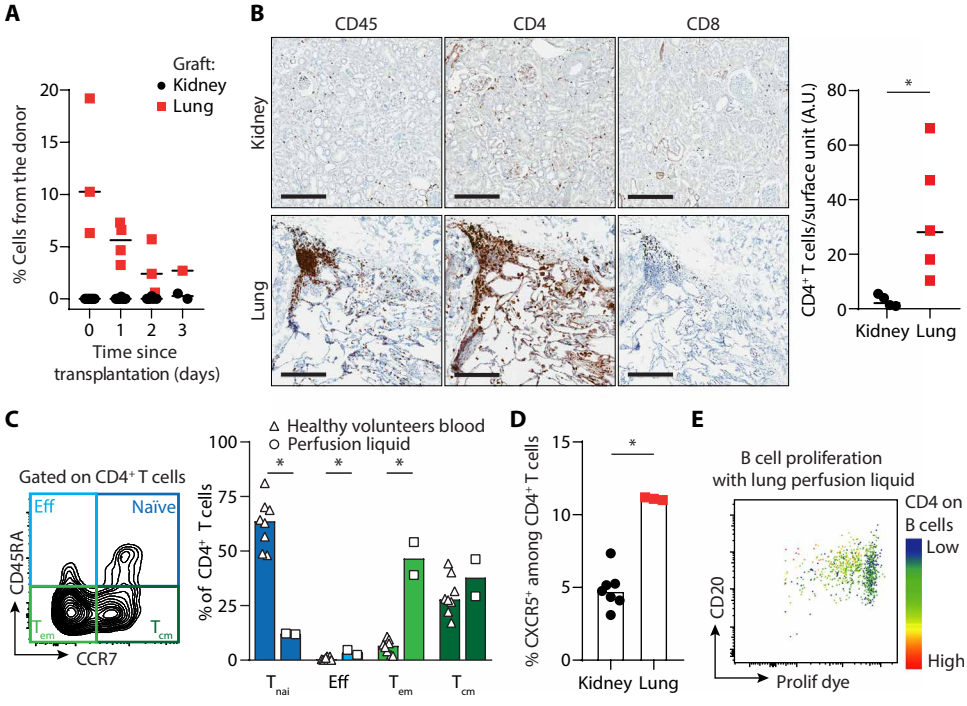

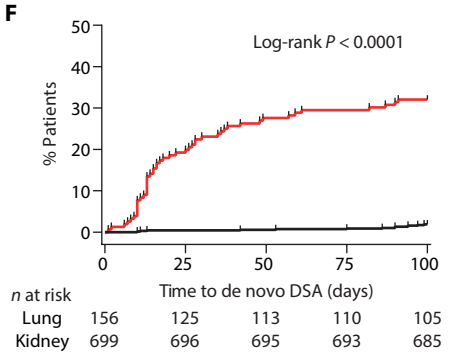

Fig. 5. Incidence of early DSA generation correlates with donor $CD4^+$ T cell frequencies contained in the graft. (**A**) The proportion of $CD3^+$ T cells of donor origin (chimerism) was evaluated in the circulation of patients at various time points after kidney or lung transplantation. Individual values are plotted. Horizontal bars indicate median values. (**B**) Left: Paraffin-embedded slides of kidney (top row) or lung (bottom row) that were stained for CD45 (left), CD4 (middle), or CD8 (right) cells. Scale bars, 300 μm. Right: The density of $CD4^+$ T cells quantified by computer-assisted morphometry and compared between kidney and lung. Horizontal bars indicate median values. Data were analyzed by Mann-Whitney test. *$P < 0.05$. (**C**) Lung graft perfusion fluids were collected at the end of the procedure, and their cell content was analyzed by flow cytometry. Left: A representative flow profile for T cell phenotyping in lung perfusion liquid. Right: The percentages of T_{nai}, Eff, T_{em}, and T_{cm} $CD4^+$ T cells detected in lung allograft perfusion fluids (open squares), which were compared with those observed in the blood of healthy volunteers (triangles). Bars indicate median values. Data were analyzed by Mann-Whitney test. *$P < 0.05$. (**D**) Kidney and lung graft perfusion fluids were collected at the end of the procedure, and their cell content was analyzed by flow cytometry. The percentage of T_{FH} ($CXCR5^+$ cells) among $CD4^+$ T cells is compared. Bars indicate median values. Data were analyzed by Mann-Whitney test. *$P < 0.05$. (**E**) The cells collected in a lung perfusion liquid were cocultured with allogeneic B cells stained with a proliferation dye. The flow cytometry plot shows the proliferation of the $CD20^+$ population. A color scale is used to code the proportion of B cells that acquired CD4 molecules by trogocytosis. (**F**) A Kaplan-Meier curve for DSA-free survival after kidney (black curve) and lung (red curve) transplantation is shown.

To evaluate whether passenger $CD4^+$ T cells could help the recipient's B cells to differentiate into DSA-producing plasma cells, the cells contained in a lung perfusion liquid were cocultured with allogeneic B cells from a healthy volunteer. As expected, T cells contained in the lung perfusion liquid interacted with B cells and efficiently promoted their proliferation (Fig. 5E). These data led us to hypothesize that, in the clinic (as in the murine model; Fig. 2G), there is a direct relationship between the amount of donor T cells found in the circulation after transplantation, the intensity of inverted direct allorecognition, and the risk to develop a first early wave of DSA. To test this, we compared the incidence of DSAs in two cohorts of lung ($n = 156$) and kidney ($n = 699$) recipients in the early phase (first 100 days) after transplantation. Patients' characteristics are summarized in table S1. As expected, lung recipients, in which inverted direct allorecognition is most likely to occur, were also much more prone to generate de novo DSA within the first 100 days ($P < 0.0001$, log-rank test; Fig. 5F).

Early onset of de novo DSAs occurs frequently after intestinal transplantation

To further evaluate the robustness of the relationship between the amount of donor T cells in the graft and the risk of developing a first early wave of DSAs, we focused our interest on intestinal transplantation. This rare procedure is currently the only therapeutic option for patients with intestinal failure with irreversible complications associated with the long-term use of parenteral nutrition (*41*). Intestinal grafts include gut-associated lymphoid tissue (GALT; Fig. 6A), a professional secondary lymphoid tissue that contains as many lymphocytes as the spleen (*42*), and germinal centers enriched in T_{FH} (Fig. 6A). We therefore hypothesized that intestinal graft recipients could experience a very strong inverted direct stimulation of their alloreactive B cells and should be at extremely high risk of developing an early DSA response. Twenty-six intestine recipients transplanted between 1 May 2009 and 30 November 2014 were retrospectively enrolled (the clinical characteristics of the patients are presented in table S1). Two patients who died within the first week after the procedure were excluded because they had no DSA screening available. In agreement with our hypothesis, 20 of 24 (83%) intestine recipients developed de novo DSAs within the first 30 days after transplantation, with a higher incidence and faster kinetics than what observed in any other types of transplantation ($P < 0.0001$ for intestine versus lung and intestine versus kidney, log-rank test; Fig. 6B).

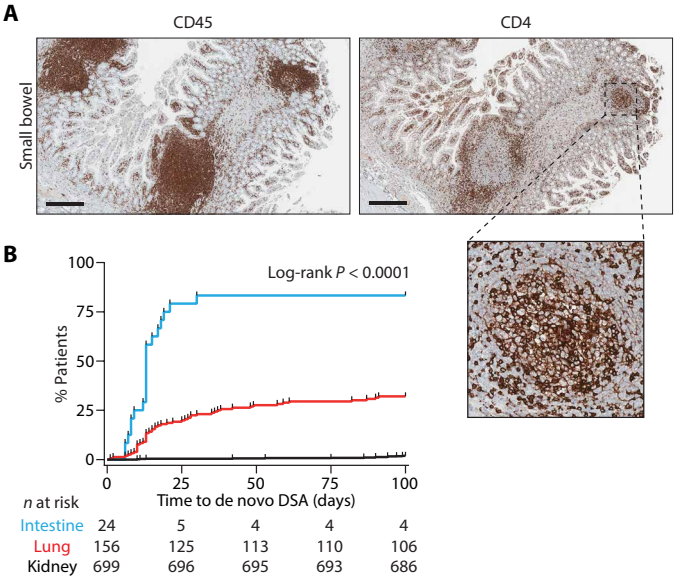

Fig. 6. Early onset of de novo DSAs is observed after intestinal transplantation. (**A**) Paraffin-embedded slides of small intestine were stained for $CD45^+$ (left) or $CD4^+$ (right) cells. The magnified image highlights the $CD4^+$ T_{FH} cell population in a germinal center. Scale bars, 500 μm. (**B**) Kaplan-Meier curves of DSA-free survival after kidney (black), lung (red), and intestinal (blue) transplantation are shown.

Early DSA responses in humans are transient

We then compared the early (<100 days; supposed to be mediated by the inverted direct pathway) and late (≥100 days; supposed to be mediated by the indirect pathway) DSA responses in our three cohorts of transplant recipients (kidney, lung, and intestine). The amount of DSAs generated was higher (fig. S6A) and the repertoire was more diverse (fig. S6B) in early than in late DSA responses. Furthermore, reminiscent of the mouse model, in which the DSA response induced by the inverted direct pathway was biased toward the donor's MHC I (Fig. 1C), the proportion of patients with anti–MHC I DSA was higher in early than in late DSA responses (fig. S6C). Another similarity with the murine model (Fig. 1, B and F) was the fact that early DSA responses exhibited a rapid decay of alloantibodies titers, whereas late DSA responses persisted over time. This observation, first made by the comparison of the early DSA responses of intestine recipients and the late DSA responses of kidney recipients (fig. S6D), held true in a homogeneous population of lung transplant recipients (fig. S6E).

Complement-binding early DSAs impair graft survival

The fact that early DSA responses are transient does question their pathogenicity for the graft and, therefore, their relevance for clinicians. There are two processes by which DSAs could damage the graft. First, the binding of circulating DSAs to graft endothelium can recruit Fcγ receptor–expressing innate immune effectors, which, in turn, promote damage to graft endothelial cells through the release of lytic enzymes (*43*). This process is slow and leads to subclinical or chronic AMR (*2*, *44*, *45*). Second, whenever the titer is sufficient, DSAs can activate the classical complement pathway, thereby accelerating the rejection process (*2*, *14*). Given the transient nature of early DSA responses, we hypothesized that the latter could affect graft survival if complement-binding DSAs were generated. We tested this hypothesis in the two cohorts of lung and intestine recipients, in which the ability of DSAs generated within the first 100 days to bind C1q in ex vivo assay was assessed. Occurrence of severe chronic lung allograft dysfunction (CLAD 3; in lung recipients; Fig. 7A) or graft survival (in intestine recipients; Fig. 7B) was compared between three groups of recipients: with non–complement-binding DSAs, with complement-binding DSAs, and without DSA. In line with our hypothesis, early DSA responses did affect intestinal graft survival only for recipients with DSAs able to activate the classical complement cascade ($P = 0.0019$ and $P = 0.0135$ for lung and intestine recipients, respectively, log-rank test).

DISCUSSION

$CD4^+$ T cell help is known to be mandatory for the differentiation of the recipient's allospecific B cells into DSA-producing plasma cells

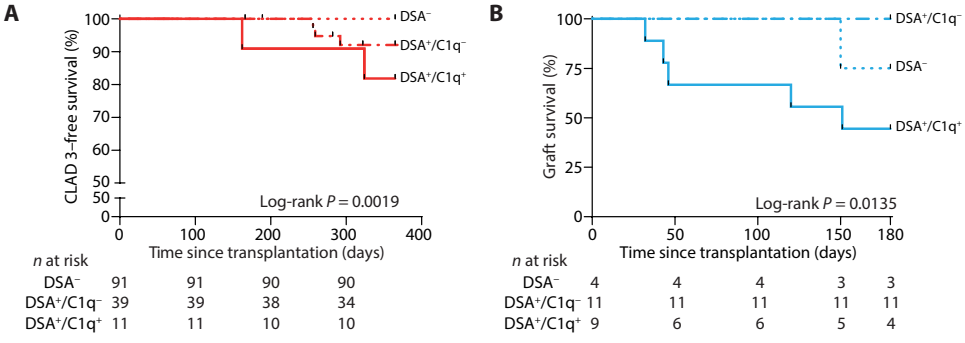

Fig. 7. Early onset of de novo DSAs has a detrimental impact on transplantation outcome. Kaplan-Meier curves for (**A**) severe chronic lung allograft dysfunction (CLAD 3)–free survival or (**B**) intestinal graft survival are shown according to the presence of early DSAs (DSA^+ or DSA^-) and their ability to bind complement ($C1q^+$ or $Cq1^-$).

(*10*–*13*). However, we here demonstrate that when graft contains sufficient number of passenger $CD4^+$ T cells, these cells migrate into the recipient's circulation and can provide help to the recipient's allospecific B cells; this was associated with an early wave of transient DSAs directed predominantly against donor-specific MHC I alloantigens. We named this pathway of allorecognition "inverted direct" because, as in canonical direct pathway, it involves recognition of allogeneic MHC molecules by the TCR of $CD4^+$ T cells in a peptide-degenerate manner. However, in this case, the T cells are from the donor, whereas the APCs (the allospecific B cells) come from the recipient. The origins of the cells are therefore inverted. The results from our murine models are aligned with experimental data reported by Harper *et al.* (*32*), and our translational approach allowed the validation of these findings in the clinical setting, suggesting that inverted direct pathway also exists in patients and might have a detrimental impact on graft survival.

The interactions between lymphohematopoietic cells from two genetically distinct patients have been previously reported in bone marrow transplantation (*46*). Although the threat of lymphohematopoietic graft-versus-host disease (*47*) is well known, other studies have also documented the beneficial impact of the bidirectional alloreactivity (graft-versus-host and host-versus-graft reactivity, due to micro- or macrochimerism) in the induction and maintenance of transplant tolerance (*48*–*50*). Even if the interaction reported here can be considered belonging to the same family of immune mechanisms, it stands out because, in contrast with previously discussed situations (*47*) in which the donor's T cells invariably destroy the recipient's cells, the inverted direct pathway instead provides functional help to the recipient's B cells.

Our results challenge the prevailing dogma that the indirect pathway is the only mechanism involved in DSA generation. In the indirect pathway, binding of donor MHC molecules to the BCR activates allospecific B cells of recipient, which, in turn, present alloantigen-derived peptides within surface MHC II molecules. Only when these complexes are recognized by the recipient's cognate $CD4^+$ T cells can the latter deliver the second signal of activation to allospecific B cells. In the inverted direct pathway, this control of the specificity of the B cell response is expected to be lost. It is the recipient MHC II molecules (expressed on all B cells irrespective of their antigen specificity) that are directly recognized by the donor's $CD4^+$ T cells of direct allospecificity. However, no massive polyclonal antibody response was observed, neither in experimental models nor in transplant recipients. The results of our experiments indicate instead that the alloantigen specificity of the response triggered by the inverted direct pathway is maintained through the requirement for BCR signal, which provides the allospecific B cell clones with a decisive advantage to interact with alloreactive donor T cells.

A notable feature of the DSA response generated through the inverted direct pathway is its transient nature. The number of $CD4^+$ T cells available to provide help being a critical factor for the development of germinal centers (*11*), it is likely that the rapid diminution in the help provided to allospecific B cells due to the elimination of donor's T cells could explain the decay in DSA titer. This hypothesis is supported by a recent experimental study, which has reported that, at 7 weeks after heart transplantation, no germinal center could be detected in the secondary lymphoid organs of recipients in which only the inverted direct pathway was operant (*51*). Pushing this line of thinking forward, the authors demonstrated that, in this murine model, the antibody response depended primarily on an extrafollicular B cell response (*51*).

The inverted direct pathway of allorecognition provides a possible molecular explanation for the early transient onset of anti–MHC I DSA sometimes observed in naïve recipients within days after transplantation, a delay too short to be the consequence of the indirect pathway. Early onset of DSA, which is rare after kidney transplantation (*16*), has been much more frequently observed in other types of transplantation, including lung (*52*, *53*) and intestinal transplantations (*21*, *54*, *55*). This is in agreement with the fact that, if passenger $CD4^+$ T cells with a tissue-resident memory phenotype can be found in almost all organs (*56*), including kidney graft (*57*, *58*), then the inverted direct pathway is much stronger when the transplanted organ contains mucosa-associated lymphoid tissue (MALT), such as BALT in the lung and GALT in the intestine. We found a correlation between the number of passenger $CD4^+$ T cells in the graft, the presence of donor $CD4^+$ T cells in the recipient's circulation, and the risk of early DSA response. Beyond the mere quantitative difference, the nature of the $CD4^+$ T cells present within the graft might also have an influence on the process. Although tissue-resident memory $CD4^+$ T cells can acquire B cell helper functions upon TCR stimulation, MALT contains a large amount of T_{FH}, a subset specialized in providing help to B cell, which constitutively express the chemokine receptor CXCR5, which is required to efficiently migrate to the recipient's B cell areas. The development of ectopic lymphoid tissue (named "tertiary" lymphoid structures) has been reported upon chronic inflammation in numerous organs normally devoid of developmentally programmed secondary lymphoid tissue (*59*–*61*). It is reasonable to speculate that such organs, when transplanted, induce inverted direct allorecognition.

Strategies to target the inverted direct pathway, and therefore limit the early generation of DSA, are needed to promote graft survival. We found passenger $CD4^+$ T cells in cold perfusion liquid; however, normothermic perfusion could be more efficient at clearing tissue-resident T cells from the graft by mobilizing them in the perfusion liquid (*62*). This technique alone is, however, likely to be insufficient to achieve adequate T cell depletion of the graft, a goal that may require

adding T cell–depleting (or T cell-attracting) drugs to the perfusion fluid (*63*). Last, it should be kept in mind that passenger $CD4^+$ T cells can only provide help to B cells if they reach the recipient's secondary lymphoid organs. In this regard, induction by thymoglobulin appears as the most straightforward option to reduce the intensity of inverted direct pathway by destroying all passenger $CD4^+$ T cells whenever they enter the recipient's circulation.

Our study has some limitations. First, the data obtained in patients, although consistent with the existence of the inverted direct pathway of allorecognition in the clinic, remain purely correlative. The demonstration that interactions between the allogeneic donor's T cells and the recipient's B cells occur in patients would have required performing invasive biopsies of secondary lymphoid organs, which are not devoid of side effects and were difficult to justify. Second, the reason why the inverted direct pathway of allorecognition triggered selectively the activation of recipient's allospecific B cells remains incompletely understood. This result is in disagreement with the data reported by Harper *et al.*, who observed the generation of autoantibodies in a murine experimental model of inverted direct allorecognition (*32*). Although we did not detect autoantibodies in our model, we cannot exclude that the difference in the molecular mechanisms controlling the specificity of B cell clones able to differentiate into plasma cells might be more leaky in the case of the inverted direct pathway and therefore responsible for the higher incidence of autoantibodies sometimes reported in transplant recipients (*64*–*66*). Last, this study did not explore what mechanisms could influence the interactions between donor and recipient hematopoietic cells toward DSA production, tolerance promotion, or graft-versus-host disease, a fascinating topic that will require future dedicated studies.

In conclusion, we describe here a mechanism of allorecognition that we named the inverted direct pathway, in which intragraft passenger $CD4^+$ T cells of donor origin provide help to the recipient's allospecific B cells. The inverted direct pathway is prominent when transplanted organs contain MALT. This mechanism thus provides a possible explanation for the particularly high incidence of early transient onset of anti–MHC I DSAs reported after transplanting such organs.

MATERIALS AND METHODS

Study design

Transplanting allogeneic heart grafts in recipient mice devoid of T cells, we observed the unexpected generation of DSAs. This murine experimental model was used to perform a mechanistic study, which led to the identification of the inverted direct allorecognition pathway. The murine model was then adapted and combined with in vitro approaches to dissect the molecular mechanisms involved in the inverted direct allorecognition pathway. When applicable, mice were randomly assigned to the different groups. The follow-up of the mice and most of the analyses were not blinded. Only the pathological analysis of the heart grafts was blinded. Sample sizes were not based on power analysis. Each experiment was performed at least twice, and data describe biological replicates. No outliers were excluded from the analysis. Aiming at evaluating the clinical validity of these experimental findings, we next analyzed perfusion liquids of renal and lung grafts to characterize their content in immune cells from donor origin and thus provide indirect clues regarding the existence of the inverted direct allorecognition pathway in patients. Three independent cohorts of patients living with a transplant (kidney, lung, or intestine) were then retrospectively analyzed to study the relation between graft's content in donor $CD4^+$ T cells and the incidence of early DSAs and graft survival.

Mice

WT C57BL/6 ($H\text{-}2^b$) and CBA ($H\text{-}2^k$) mice were purchased from Charles River Laboratories. MHC II KO (AßKO) mice on C57BL/6 genetic background were provided by C. Benoist and D. Mathis (*67*). CD3εKO mice on C57BL/6 genetic background were purchased from the Jackson Laboratory. Rag2KO mice on a C57BL/6 background were obtained from the Cryopreservation Distribution Typage et Archivage Animal. All mice were maintained under EOPS (Exemption of Specific Pathogenic Organisms) conditions in our animal facility: Plateau de Biologie Expérimentale de la Souris (www.sfr-biosciences.fr/plateformes/animal-sciences/AniRA-PBES). All studies and procedures were performed in accordance with European Union guidelines and were approved by the local ethical committee for animal research (CECCAPP Lyon, registered by the French National Ethics Committee of Animal Experimentation under no. C2EA15; www.sfr-biosciences.fr/ethique/experimentation-animale/ceccapp).

Heterotopic heart transplantation in mice

Heart transplantations were performed as previously described (*3*, *68*). We used intravenous administration of 17A2 (20 μg), an anti-murine CD3 mAb (*69*), and GK1.5 (32 μg), an anti-murine CD4 mAb (*70*) (both rat IgG2b antibodies), to deplete $CD3^+$ or $CD4^+$ T cells in mice. The injections were given to the donors 2 days in a row, just before the transplantation (17A2) or 1 week before the transplantation (GK1.5). The recipients were depleted by two injections, the day of the transplantation and the following day. DSA titers were determined using a single antigen bead assay or a custom flow cross-match assay as in the study by Chen *et al.* (*3*). For further details, see Supplementary Methods and fig. S7.

Pathological analyses

Cardiac transplants were collected for the histological assessment of the DSA-mediated lesions. Recipient mice were euthanized by cervical dislocation after general anesthesia. Heart transplants were fixed in 4% buffered formalin for 24 hours and embedded in paraffin for hematoxylin and eosin staining. The slides were scanned before analysis (NanoZoomer S60 digital slide scanner, Hamamatsu Photonics). Regions for analysis were randomly selected in the left ventricle.

Intravenous allogeneic cell injection

Purified allogeneic CBA ($H\text{-}2^k$) $CD4^+$ T cells (2×10^5 to 5×10^6) were injected intravenously to CD3εKO, Rag2KO, or WT C57BL/6 ($H\text{-}2^b$) mice. The day before the T cell transfer, 5×10^6 B cells purified from WT or AβKO mice ($H\text{-}2^b$) were injected intravenously to Rag2KO mice. $CD4^+$ T cells and B cells were isolated using negative selection kits (STEMCELL Technologies and R&D Systems), according to the manufacturer's instructions. For some experiments, $CD4^+$ T cells were fixed with 35% ethanol before injection.

Cocultures

To perform murine cell cultures, spleens were harvested from C57BL/6, CBA, and AβKO mice. B cells from C57BL/6 or AβKO mice and T cells from C57BL/6 and CBA mice were isolated, using B and T cell negative selection kits (R&D Systems), respectively, according to the manufacturer's instructions. For B cell proliferation assays, B cells were stained with a proliferation dye (CellTrace Violet, Thermo

Fisher Scientific) according to the manufacturer's instructions. B cells (10^5) were cocultured with 10^5 syngeneic or allogeneic T cells in the presence or absence of a soluble anti-κ mAb (1 μg for 10^6 cells; see Supplementary Methods). When indicated, an anti-CD154 mAb was added (clone MR1, BD Biosciences; 10 μg/ml).

For MHC expression assays, 10^6 B cells from C57BL/6 mice were cultured overnight at 37°C and 5% CO_2 in complete medium [for mouse: RPMI 1640 GlutaMAX medium (Invitrogen) supplemented with 10% fetal calf serum, 50 μM β-mercaptoethanol (Sigma-Aldrich), 25 mM Hepes (Invitrogen), and penicillin/streptomycin (10 U/ml; Invitrogen)], with a soluble anti-κ mAb (1 μg for 10^6 cells).

Before staining, murine cells were incubated with a blocking anti-mouse Fc receptor antibody (2.4G2; homemade hybridoma). Cells were then incubated at 4°C with the following fluorescent antibodies: CD3 [dilution 1:200; 145-2C11, Brilliant Violet 421 (BV421), BD Biosciences, catalog no. 562600, RRID:AB_11153670], CD19 [dilution 1:200; 1D3, phycoerythrin (PE)–CF594, BD Biosciences, catalog no. 562291, RRID:AB_11154223], B220 (dilution 1:200; RA3-6B2, allophycocyanin, BD Biosciences, catalog no. 553092, RRID:AB_398531), and MHC II [dilution 1:250; 2G9, fluorescein isothiocyanate (FITC), BD Biosciences, catalog no. 553623, RRID:AB_394958]. Before analysis by flow cytometry, DAPI (4′,6-diamidino-2-phenylindole dihydrochloride; Sigma-Aldrich) was added to the cell suspension to exclude dead cells. Samples were analyzed on a BD LSR II flow cytometer (BD Biosciences).

Human PBMCs were collected from the French National Blood Service (Etablissement Français du Sang, EFS) and isolated by centrifugation on a Ficoll density gradient. B cells and T cells were isolated, using B and T cell negative selection kits (R&D Systems), respectively, according to the manufacturer's instructions. For MHC, CD40, CD86, and CD80 expression assays, 5×10^5 PBMC cells were cultured overnight at 37°C and 5% CO_2 in complete medium [for human: RPMI 1640 GlutaMAX medium (Invitrogen) supplemented with 10% fetal calf serum, 25 mM Hepes (Invitrogen), and penicillin/streptomycin (10 U/ml; Invitrogen)], with a soluble anti-human IgM $F(ab')_2$ (5 μg/ml). Cells were then processed as described above for murine samples.

For human B cell proliferation assays, T cells and B cells were purified (up to 95% purity) from PBMCs by negative selection with magnetic enrichment kits (R&D Systems). B cells were stained with a proliferation dye (CellTrace Violet or carboxyfluorescein succinimidyl ester, Thermo Fisher Scientific) according to the manufacturer's instructions. B cells (4×10^5) were cocultured with 4×10^4 syngeneic or allogeneic T cells in the presence or absence of a soluble anti-human IgM $F(ab')_2$ (5 μg/ml; Jackson ImmunoResearch).

Cells were then incubated at 4°C with the following fluorescent antibodies: CD3 [dilution 1:20; UHCT1, PE, BD Biosciences, catalog no. 555333, RRID:AB_395740 or peridinin-chlorophyll-protein (PerCP)–cyanin 5.5 (Cy5.5), BD Biosciences, catalog no. 560835, RRID:AB_2033956], CD4 (dilution 1:40; SK3, PE-Cy7, BD Biosciences, catalog no. 557852, RRID:AB_396897), CD19 (dilution 1:40; HIB19, allophycocyanin-R700, BD Biosciences, catalog no. 564977, RRID:AB_2744308), CD20 (2H7; dilution 1:5; FITC, BD Biosciences, catalog no. 555622, RRID:AB_395988; or dilution 1:40; BV421, BD Biosciences, catalog no. 562873, RRID:AB_2737857), MHC II (dilution 1:20; G46-6, allophycocyanin-H7, BD Biosciences, catalog no. 561358, RRID:AB_10611876), CD40 (dilution 1:20; 5C3, Alexa Fluor 488, BioLegend, catalog no. 334318, RRID:AB_1501188), CD86 (dilution 1:20; FUN-1, BV650, BD Biosciences, catalog no. 563411, RRID:AB_2744456), CD80 (dilution 1:20; 2D10, PE/Dazzle 594, BioLegend, catalog no. 305230, RRID:AB_2566489), and a Fixable Viability Dye (dilution 1:500; eBioscience, eFluor506). Samples were analyzed on a BD LSRFortessa 4L flow cytometer (BD Biosciences).

Cohorts of transplant recipients

The renal and lung transplant cohort studies were carried out in accordance with French legislation on biomedical research and the Declaration of Helsinki. All patients gave informed consent for the utilization of clinical data [Données Informatiques Validées en Transplantation (DIVAT)] and biological samples for research purpose. For DIVAT, a declaration was made to the CCTIRS (Comité consultatif sur le Traitement de l'Information en matière de Recherche dans le domaine de la Santé) and the CNIL (Commission nationale de l'Informatique et des Libertés). For the biocollection, an authorization (nos. of biocollection: AC-2011-1375 and AC-2016-2706) was obtained from the French Ministry of Higher Education and Research (direction générale pour la recherche et l'innovation, cellule bioéthique). For the study of the early incidence of DSAs after transplantation, all patients over 16 years who underwent a first lung transplantation at Bichat (Paris, France), Foch (Suresnes, France), or Marie-Lannelongue (le Plessis-Robinson, France) hospitals between 1 May 2008 and 30 June 2012 or a first kidney transplantation at Lyon University Hospital (Lyon, France) between 1 January 2013 and 31 December 2017 were enrolled. The analysis compared the period of the first 100 days with the subsequent period. This period allows for the inclusion of the anti-HLA antibody testing carried out in the third month after transplantation, which corresponds to the first sampling for many patients. For the lung transplant survival study, the outcome considered the onset of severe CLAD 3. For the intestine transplant cohort, all patients who underwent intestinal transplantation at Necker University Hospital (Paris) between 1 May 2009 and 30 November 2014 were enrolled. For the intestinal transplant survival study, the outcome considered both graft and patient survival.

Analysis of graft perfusion liquids

The renal and lung perfusion liquids (from Lyon University Hospital and Bichat University Hospital, Paris, respectively) were collected after the organ was removed from the machine. The cells were isolated as follows: after a first wash in phosphate-buffered saline (PBS), leukocytes and red blood cells were counted before red blood cell lysis in ammonium-chloride-potassium (ACK) lysis buffer (for renal perfusion liquids only). After a second wash in PBS, cells were frozen and kept at −80°C until their analysis. After thawing, the cells were cultured for 12 hours in complete RPMI 1640 at 37°C and 5% CO_2 before staining, with or without human T-activator CD3/CD28 Dynabeads (Thermo Fisher Scientific). Cells were then incubated at 4°C with relevant antibodies: CD3 (dilution 1:100; UCHT1, BV421, BD Biosciences, catalog no. 562426, RRID:AB_11152082), CD4 (dilution 1:80; SK3, PerCP-Cy5.5, BD Biosciences, catalog no. 332772, RRID:AB_2868621), CD8 (dilution 1:100; SK1, allophycocyanin-H7, BD Biosciences, catalog no. 560179, RRID:AB_1645481), CXCR5 (dilution 1:80; RF8B2, Alexa Fluor 647, BD Biosciences, catalog no. 558113, RRID: AB_2737606), CD40L (dilution 1:20; TRAP1, PE, BD Biosciences, catalog no. 561720, RRID:AB_10924597), CD45RA (dilution 1:100; L48, PE-Cy7, BD Biosciences, catalog no. 337186, RRID:AB_2828012), CCR7 (dilution 1:40; 150503, FITC, BD Biosciences,

catalog no. 561271, RRID:AB_10561679; or dilution 1:20; 3D12, BV605, BD Biosciences, catalog no. 563711, RRID:AB_2738385), ICOS (dilution 1:20; ISA-3, FITC, Thermo Fisher Scientific, catalog no. 11-9948-41, RRID:AB_10667883), and a viability dye LIVE/DEAD Aqua (1:1000; Invitrogen). Cells were then fixed using Cytofix/Cytoperm (BD Biosciences) according to the manufacturer's instructions. Samples were acquired on a BD FACSAria II flow cytometer (BD Biosciences) or a BD LSRFortessa 4L flow cytometer (BD Biosciences). Data were analyzed with FlowJo software (Tree Star).

Kidney, lung, and intestinal graft histology

The samples analyzed by histology were kidneys that were discarded for transplantation or lungs and intestines from cancer excision surgery. In the latter case, the samples tested were distant from any tumor lesions. CD45, CD4, and CD8 staining were performed by automated immunohistochemistry (System BenchMark ULTRA IHC/ISH, Roche) using anti-human CD45 (dilution 1:100; 2B11 and PD7/26, Dako), CD4 (dilution 1:100; SP35, Cell Marque), and CD8 (dilution 1:20; 4B11, Novocastra) mAbs and the ultraView Universal DAB Detection Kit (Ventana Medical Systems). Computer-assisted morphometric quantifications were performed using FIJI software (*71*).

Analysis of PBMC chimerism after transplantation

Donor and recipient leukocyte chimerism was evaluated in PBMCs isolated from kidney and lung transplant recipients. Samples were taken on day 0 just after transplantation surgery and at day 1, day 2, and day 3 after transplantation. Chimerism was performed on genomic DNA extracted from CD3 cells after cell sorting (MACSprep Chimerism CD3 MicroBeads, human, Miltenyi Biotech) using quantitative real-time polymerase chain reaction associated with TaqMan technology. Before quantification, the donor and recipient were genotyped using primers and probes specific for 34 genetic markers (QTRACE Assays, JETA Molecular). An allele was considered informative when positive on recipient DNA and negative on donor DNA or conversely negative on recipient DNA and positive on donor DNA. Then, quantification was performed, and the result was given as a percentage of donor cells on patient posttransplantation samples, based on the donor informative system as reference. Mixed chimerism was defined by the presence of at least 0.2% of donor cells.

Anti-HLA antibody detection and characterization

Collected serum samples were analyzed using a single-antigen bead assay (Immucor or One Lambda). DSAs were defined as positive by a mean fluorescence intensity (MFI) greater than 500. The C1q-fixing capacity of posttransplantation DSAs was measured using the C1q-Screen kit (One Lambda), according to the manufacturer's recommendations. The ability of antibodies to bind C1q is correlated to their titers (fig. S8A). A receiver operating characteristic curve was constructed with all available C1q assays (area under the curve = 0.929; 95% confidence interval 0.876 to 0.983; fig. S8B). Given this high value, these data were used to define a test threshold above which DSAs were considered as complement fixing (MFI = 3040; see fig. S8, A and B). This threshold was used to extrapolate the results of the C1q assay for the patients whose serum samples were not available for the retrospective C1q analysis.

Statistical analysis

All raw, individual-level data for experiments where $n < 20$ are presented in data file S1. Statistical analysis and graphs were performed using Prism software (GraphPad). Quantitative DSA titers were compared using multiple unpaired *t* tests. All other quantitative variables were expressed as median ± IQR and compared using Mann-Whitney tests. All tests were two-sided. Incidence and survival data were analyzed by Kaplan-Meier plot and compared using a log-rank test. Statistical significance was considered for a P value of <0.05.

SUPPLEMENTARY MATERIALS

stm.sciencemag.org/cgi/content/full/14/663/eabg1046/DC1
Methods
Figs. S1 to S8
Table S1
Data file S1
MDAR Reproducibility Checklist

View/request a protocol for this paper from *Bio-protocol*.

REFERENCES AND NOTES

1. J. Sellarés, D. G. de Freitas, M. Mengel, J. Reeve, G. Einecke, B. Sis, L. G. Hidalgo, K. Famulski, A. Matas, P. F. Halloran, Understanding the causes of kidney transplant failure: The dominant role of antibody-mediated rejection and nonadherence. *Am. J. Transplant.* **12**, 388–399 (2012).
2. E. Pouliquen, A. Koenig, C. C. Chen, A. Sicard, M. Rabeyrin, E. Morelon, V. Dubois, O. Thaunat, Recent advances in renal transplantation: Antibody-mediated rejection takes center stage. *F1000prime Rep.* **7**, –51 (2015).
3. C.-C. Chen, E. Pouliquen, A. Broisat, F. Andreata, M. Racapé, P. Bruneval, L. Kessler, M. Ahmadi, S. Bacot, C. Saison-Delaplace, M. Marcaud, J.-P. D. Van Huyen, A. Loupy, J. Villard, S. Demuylder-Mischler, T. Berney, E. Morelon, M.-K. Tsai, M.-N. Kolopp-Sarda, A. Koenig, V. Mathias, S. Ducreux, C. Ghezzi, V. Dubois, A. Nicoletti, T. Defrance, O. Thaunat, Endothelial chimerism and vascular sequestration protect pancreatic islet grafts from antibody-mediated rejection. *J. Clin. Invest.* **128**, 219–232 (2018).
4. O. Thaunat, Humoral immunity in chronic allograft rejection: Puzzle pieces come together. *Transpl. Immunol.* **26**, 101–106 (2012).
5. J. H. Y. Siu, V. Surendrakumar, J. A. Richards, G. J. Pettigrew, T cell allorecognition pathways in solid organ transplantation. *Front. Immunol.* **9**, 2548 (2018).
6. B. Afzali, G. Lombardi, R. I. Lechler, Pathways of major histocompatibility complex allorecognition. *Curr. Opin. Organ Transplant.* **13**, 438–444 (2008).
7. F. G. Lakkis, R. I. Lechler, Origin and biology of the allogeneic response. *Cold Spring Harb. Perspect. Med.* **3**, a014993 (2013).
8. E. J. Suchin, P. B. Langmuir, E. Palmer, M. H. Sayegh, A. D. Wells, L. A. Turka, Quantifying the frequency of alloreactive T cells in vivo: New answers to an old question. *J. Immunol.* **166**, 973–981 (2001).
9. P. F. Halloran, J. Chang, K. Famulski, L. G. Hidalgo, I. D. R. Salazar, M. Merino Lopez, A. Matas, M. Picton, D. de Freitas, J. Bromberg, D. Serón, J. Sellarés, G. Einecke, J. Reeve, Disappearance of T cell-mediated rejection despite continued antibody-mediated rejection in late kidney transplant recipients. *J. Am. Soc. Nephrol* **26**, 1711–1720 (2015).
10. D. J. Steele, T. M. Laufer, S. T. Smiley, Y. Ando, M. J. Grusby, L. H. Glimcher, H. Auchincloss Jr., Two levels of help for B cell alloantibody production. *J. Exp. Med.* **183**, 699–703 (1996).
11. C.-C. Chen, A. Koenig, C. Saison, S. Dahdal, G. Rigault, T. Barba, M. Taillardet, D. Chartoire, M. Ovize, E. Morelon, T. Defrance, O. Thaunat, CD4+ T cell help is mandatory for naive and memory donor-specific antibody responses: Impact of therapeutic immunosuppression. *Front. Immunol.* **9**, 275 (2018).
12. S. Dahdal, C. Saison, M. Valette, E. Bachy, N. Pallet, B. Lina, A. Koenig, G. Monneret, T. Defrance, E. Morelon, O. Thaunat, Residual activatability of circulating Tfh17 predicts humoral response to thymodependent antigens in patients on therapeutic immunosuppression. *Front. Immunol.* **9**, 3178 (2019).
13. T. M. Conlon, K. Saeb-Parsy, J. L. Cole, R. Motallebzadeh, M. S. Qureshi, S. Rehakova, M. C. Negus, C. J. Callaghan, E. M. Bolton, J. A. Bradley, G. J. Pettigrew, Germinal center alloantibody responses are mediated exclusively by indirect-pathway CD4 T follicular helper cells. *J. Immunol.* **188**, 2643–2652 (2012).
14. A. Sicard, S. Ducreux, M. Rabeyrin, L. Couzi, B. McGregor, L. Badet, J. Y. Scoazec, T. Bachelet, S. Lepreux, J. Visentin, P. Merville, V. Fremeaux-Bacchi, E. Morelon, J.-L. Taupin, V. Dubois, O. Thaunat, Detection of C3d-binding donor-specific anti-HLA antibodies at diagnosis of humoral rejection predicts renal graft loss. *J. Am. Soc. Nephrol.* **26**, 457–467 (2015).
15. R. S. Gaston, J. M. Cecka, B. L. Kasiske, A. M. Fieberg, R. Leduc, F. C. Cosio, S. Gourishankar, J. Grande, P. Halloran, L. Hunsicker, R. Mannon, D. Rush, A. J. Matas, Evidence for antibody-mediated injury as a major determinant of late kidney allograft failure. *Transplantation* **90**, 68–74 (2010).

16. C. Wiebe, I. W. Gibson, T. D. Blydt-Hansen, M. Karpinski, J. Ho, L. J. Storsley, A. Goldberg, P. E. Birk, D. N. Rush, P. W. Nickerson, Evolution and clinical pathologic correlations of de novo donor-specific HLA antibody post kidney transplant. *Am. J. Transplant.* **12**, 1157–1167 (2012).
17. L. J. Lobo, R. M. Aris, J. Schmitz, I. P. Neuringer, Donor-specific antibodies are associated with antibody-mediated rejection, acute cellular rejection, bronchiolitis obliterans syndrome, and cystic fibrosis after lung transplantation. *J. Heart Lung Transplant.* **32**, 70–77 (2013).
18. R. D. Yusen, L. B. Edwards, A. I. Dipchand, S. B. Goldfarb, A. Y. Kucheryavaya, B. J. Levvey, L. H. Lund, B. Meiser, J. W. Rossano, J. Stehlik; International Society for Heart and Lung Transplantation, The Registry of the International Society for Heart and Lung Transplantation: Thirty-third Adult Lung and Heart-Lung Transplant Report-2016; Focus theme: Primary diagnostic indications for transplant. *J. Heart Lung Transplant.* **35**, 1170–1184 (2016).
19. K. M. Abu-Elmagd, G. Wu, G. Costa, J. Lunz, L. Martin, D. A. Koritsky, N. Murase, W. Irish, A. Zeevi, Preformed and de novo donor specific antibodies in visceral transplantation: Long-term outcome with special reference to the liver. *Am. J. Transplant.* **12**, 3047–3060 (2012).
20. E. Y. Cheng, M. J. Everly, H. Kaneku, N. Banuelos, L. J. Wozniak, R. S. Venick, E. A. Marcus, S. V. McDiarmid, R. W. Busuttil, P. I. Terasaki, D. G. Farmer, Prevalence and clinical impact of donor-specific alloantibody among intestinal transplant recipients. *Transplantation* **101**, 873–882 (2017).
21. M. Rabant, M. Racapé, L.-M. Petit, J. L. Taupin, O. Aubert, J. Bruneau, P. Barbet, O. Goulet, C. Chardot, C. Suberbielle, F. Lacaille, D. Canioni, J.-P. D. V. Huyen, Antibody-mediated rejection in pediatric small bowel transplantation: Capillaritis is a major determinant of C4d positivity in intestinal transplant biopsies. *Am. J. Transplant.* **18**, 2250–2260 (2018).
22. X. Zhao, G. Huang, S. Randhawa, G. Zeng, J. Lunz, P. Randhawa, Rejection of the renal allograft in the absence of demonstrable antibody and complement. *Transplantation* **101**, 395–401 (2017).
23. L. R. Solomon, S. Martin, C. D. Short, W. Lawler, R. Gokal, R. W. G. Johnson, N. P. Mallick, Late cellular rejection in renal transplant recipients. *Transplantation* **41**, 262–264 (1986).
24. H. P. Brunner-La Rocca, J. Schneider, A. Künzli, M. Turina, W. Kiowski, Cardiac allograft rejection late after transplantation is a risk factor for graft coronary artery disease. *Transplantation* **65**, 538–543 (1998).
25. O. B. Herrera, D. Golshayan, R. Tibbott, F. S. Ochoa, M. J. James, F. M. Marelli-Berg, R. I. Lechler, A novel pathway of alloantigen presentation by dendritic cells. *J. Immunol.* **173**, 4828–4837 (2004).
26. V. Russo, D. Zhou, C. Sartirana, P. Rovere, A. Villa, S. Rossini, C. Traversari, C. Bordignon, Acquisition of intact allogeneic human leukocyte antigen molecules by human dendritic cells. *Blood* **95**, 3473–3477 (2000).
27. J. Marino, M. H. Babiker-Mohamed, P. Crosby-Bertorini, J. T. Paster, C. LeGuern, S. Germana, R. Abdi, M. Uehara, J. I. Kim, J. F. Markmann, G. Tocco, G. Benichou, Donor exosomes rather than passenger leukocytes initiate alloreactive T cell responses after transplantation. *Sci. Immunol.* **1**, aaf8759 (2016).
28. Q. Liu, D. M. Rojas-Canales, S. J. Divito, W. J. Shufesky, D. B. Stolz, G. Erdos, M. L. G. Sullivan, G. A. Gibson, S. C. Watkins, A. T. Larregina, A. E. Morelli, Donor dendritic cell-derived exosomes promote allograft-targeting immune response. *J. Clin. Invest.* **126**, 2805–2820 (2016).
29. L. A. Smyth, R. I. Lechler, G. Lombardi, Continuous acquisition of MHC:peptide complexes by recipient cells contributes to the generation of anti-graft CD8+ T cell immunity. *Am. J. Transplant.* **17**, 60–68 (2017).
30. S. J. F. Harper, J. M. Ali, E. Wlodek, M. C. Negus, I. G. Harper, M. Chhabra, M. S. Qureshi, M. Mallik, E. Bolton, J. A. Bradley, G. J. Pettigrew, CD8 T-cell recognition of acquired alloantigen promotes acute allograft rejection. *Proc. Natl. Acad. Sci.* **112**, 12788–12793 (2015).
31. A. D. Hughes, D. Zhao, H. Dai, K. I. Abou-Daya, R. Tieu, R. Rammal, A. L. Williams, D. P. Landsittel, W. D. Shlomchik, A. E. Morelli, M. H. Oberbarnscheidt, F. G. Lakkis, Cross-dressed dendritic cells sustain effector T cell responses in islet and kidney allografts. *J. Clin. Invest.* **130**, 287–294 (2020).
32. I. G. Harper, J. M. Ali, S. J. F. Harper, E. Wlodek, J. Alsughayyir, M. C. Negus, M. S. Qureshi, R. Motalleb-Zadeh, K. Saeb-Parsy, E. M. Bolton, J. A. Bradley, M. R. Clatworthy, T. M. Conlon, G. J. Pettigrew, Augmentation of recipient adaptive alloimmunity by donor passenger lymphocytes within the transplant. *Cell Rep.* **15**, 1214–1227 (2016).
33. J. Gordon, A. Katira, M. Holder, I. MacDonald, J. Pound, Central role of CD40 and its ligand in B lymphocyte responses to T-dependent antigens. *Cell. Mol. Biol. (Noisy-le-grand)* **40** (Suppl 1), 1–13 (1994).
34. C. Lagresle, P. Mondière, C. Bella, P. H. Krammer, T. Defrance, Concurrent engagement of CD40 and the antigen receptor protects naive and memory human B cells from APO-1/Fas-mediated apoptosis. *J. Exp. Med.* **183**, 1377–1388 (1996).
35. T. Rothstein, J. Wang, D. Panka, L. Foote, Z. Wang, B. Stanger, H. Cui, S. Ju, A. Marshak-Rothstein, Protection against Fas-dependent Th1-mediated apoptosis by antigen receptor engagement in B cells. *Nature* **374**, 163–165 (1995).
36. E. Joly, D. Hudrisier, What is trogocytosis and what is its purpose? *Nat. Immunol.* **4**, 815–815 (2003).
37. R. J. Scothorne, Lymphatic repair and the genesis of homograft immunity. *Ann. N. Y. Acad. Sci.* **73**, 673–675 (1958).
38. P. Málek, J. Vrubel, J. Kolc, Lymphatic aspects of experimental and clinical renal transplantation. *Bull. Soc. Int. Chir.* **28**, 110–114 (1969).
39. C. P. Larsen, P. J. Morris, J. M. Austyn, Migration of dendritic leukocytes from cardiac allografts into host spleens. A novel pathway for initiation of rejection. *J. Exp. Med.* **171**, 307–314 (1990).
40. M. D. Gunn, V. N. Ngo, K. M. Ansel, E. H. Ekland, J. G. Cyster, L. T. Williams, A B-cell-homing chemokine made in lymphoid follicles activates Burkitt's lymphoma receptor-1. *Nature* **391**, 799–803 (1998).
41. D. Grant, K. Abu-Elmagd, G. Mazariegos, R. Vianna, A. Langnas, R. Mangus, D. G. Farmer, F. Lacaille, K. Iyer, T. Fishbein, Intestinal Transplant Registry Report: Global activity and trends. *Am. J. Transplant.* **15**, 210–219 (2015).
42. C. A. Janeway, P. Travers, M. Walport, M. J. Shlomchik, The mucosal immune system, in *Immunobiology: The Immune System in Health and Disease* (Garland Science, ed. 5, 2001).
43. T. Hirohashi, C. M. Chase, P. Della Pelle, D. Sebastian, A. Alessandrini, J. C. Madsen, P. S. Russell, R. B. Colvin, A novel pathway of chronic allograft rejection mediated by NK cells and alloantibody. *Am. J. Transplant. Off. J. Am. Soc. Transplant. Am. Soc. Transpl. Surg.* **12**, 313–321 (2012).
44. T. Hirohashi, S. Uehara, C. M. Chase, P. DellaPelle, J. C. Madsen, P. S. Russell, R. B. Colvin, Complement independent antibody-mediated endarteritis and transplant arteriopathy in mice. *Am. J. Transplant.* **10**, 510–517 (2010).
45. G. Guidicelli, F. Guerville, S. Lepreux, C. Wiebe, O. Thaunat, V. Dubois, J. Visentin, T. Bachelet, E. Morelon, P. Nickerson, P. Merville, J.-L. Taupin, L. Couzi, Non-complement-binding de novo donor-specific anti-HLA antibodies and kidney allograft survival. *J. Am. Soc. Nephrol. JASN.* **27**, 615–625 (2016).
46. M. Sykes, M. A. Sheard, D. H. Sachs, Graft-versus-host-related immunosuppression is induced in mixed chimeras by alloresponses against either host or donor lymphohematopoietic cells. *J. Exp. Med.* **168**, 2391–2396 (1988).
47. K. Vincent, D.-C. Roy, C. Perreault, Next-generation leukemia immunotherapy. *Blood* **118**, 2951–2959 (2011).
48. W. J. Burlingham, G. Benichou, Bidirectional alloreactivity. *Chimerism* **3**, 29–36 (2012).
49. J. Zuber, S. Rosen, B. Shonts, B. Sprangers, T. M. Savage, S. Richman, S. Yang, S. P. Lau, S. DeWolf, D. Farber, G. Vlad, E. Zorn, W. Wong, J. Emond, B. Levin, M. Martinez, T. Kato, M. Sykes, Macrochimerism in intestinal transplantation: Association with lower rejection rates and multivisceral transplants, without GVHD. *Am. J. Transplant.* **15**, 2691–2703 (2015).
50. J. Fu, J. Zuber, M. Martinez, B. Shonts, A. Obradovic, H. Wang, S. Lau, A. Xia, E. E. Waffarn, K. Frangaj, T. M. Savage, M. T. Simpson, S. Yang, X. V. Guo, M. Miron, T. Senda, K. Rogers, A. Rahman, S. Ho, Y. Shen, A. Griesemer, D. L. Farber, T. Kato, M. Sykes, Human intestinal allografts contain functional hematopoietic stem and progenitor cells that are maintained by a circulating pool. *Cell Stem Cell.* **24**, 227–239.e8 (2019).
51. M. S. Qureshi, J. Alsughayyir, M. Chhabra, J. M. Ali, M. J. Goddard, C. A. Devine, T. M. Conlon, M. A. Linterman, R. Motallebzadeh, G. J. Pettigrew, Germinal center humoral autoimmunity independently mediates progression of allograft vasculopathy. *J. Autoimmun.* **98**, 44–58 (2019).
52. F. Ius, W. Sommer, I. Tudorache, C. Kühn, M. Avsar, T. Siemeni, J. Salman, M. Hallensleben, D. Kieneke, M. Greer, J. Gottlieb, A. Haverich, G. Warnecke, Early donor-specific antibodies in lung transplantation: Risk factors and impact on survival. *J. Heart Lung Transplant.* **33**, 1255–1263 (2014).
53. R. R. Hachem, M. Kamoun, M. M. Budev, M. Askar, V. N. Ahya, J. C. Lee, D. J. Levine, M. S. Pollack, G. S. Dhillon, D. Weill, K. B. Schechtman, L. E. Leard, J. A. Golden, L. Baxter-Lowe, T. Mohanakumar, D. B. Tyan, R. D. Yusen, Human leukocyte antigens antibodies after lung transplantation: Primary results of the HALT study. *Am. J. Transplant.* **18**, 2285–2294 (2018).
54. C. Kubal, R. Mangus, R. Saxena, A. Lobashevsky, N. Higgins, J. Fridell, A. J. Tector, Prospective monitoring of donor-specific anti-HLA antibodies after intestine/multivisceral transplantation: Significance of de novo antibodies. *Transplantation* **99**, e49 (2015).
55. J. Zuber, B. Shonts, S.-P. Lau, A. Obradovic, J. Fu, S. Yang, M. Lambert, S. Coley, J. Weiner, J. Thome, S. DeWolf, D. L. Farber, Y. Shen, S. Caillat-Zucman, G. Bhagat, A. Griesemer, M. Martinez, T. Kato, M. Sykes, Bidirectional intragraft alloreactivity drives the repopulation of human intestinal allografts and correlates with clinical outcome. *Sci. Immunol.* **1**, eaah3732 (2016).
56. D. L. Turner, C. L. Gordon, D. L. Farber, Tissue-resident T cells, in situ immunity and transplantation. *Immunol. Rev.* **258**, 150–166 (2014).

57. J. Zuber, O. Boyer, B. Neven, I. Jollet, V. Renac, R. Berthaud, R. Levy, B. Lamarthée, J. Visentin, A. Marchal, N. Gouge-Biebuyck, A. Godron-Dubrasquet, N. Aladjidi, M. O. Rabah, S. Winter, J. Léon, M. Dussiot, M. Rabant, S. Krid, P. Krug, M. Charbit, F. Lacaille, I. André, M. Cavazzana, B. Llanas, L. Allard, F. Pirenne, S. Gross, R. Djoudi, P. Tiberghien, J.-L. Taupin, S. Blanche, R. Salomon, Donor-targeted serotherapy as a rescue therapy for steroid-resistant acute GVHD after HLA-mismatched kidney transplantation. *Am. J. Transplant.* **20**, 2243–2253 (2020).
58. B. J. Stewart, J. R. Ferdinand, M. D. Young, T. J. Mitchell, K. W. Loudon, A. M. Riding, N. Richoz, G. L. Frazer, J. U. L. Staniforth, F. A. V. Braga, R. A. Botting, D.-M. Popescu, R. Vento-Tormo, E. Stephenson, A. Cagan, S. J. Farndon, K. Polanski, M. Efremova, K. Green, M. D. C. Velasco-Herrera, C. Guzzo, G. Collord, L. Mamanova, T. Aho, J. N. Armitage, A. C. P. Riddick, I. Mushtaq, S. Farrell, D. Rampling, J. Nicholson, A. Filby, J. Burge, S. Lisgo, S. Lindsay, M. Bajenoff, A. Y. Warren, G. D. Stewart, N. Sebire, N. Coleman, M. Haniffa, S. A. Teichmann, S. Behjati, M. R. Clatworthy, Spatiotemporal immune zonation of the human kidney. *Science* **365**, 1461–1466 (2019).
59. A. Koenig, O. Thaunat, Lymphoid neogenesis and tertiary lymphoid organs in transplanted organs. *Front. Immunol.* **7**, 646 (2016).
60. O. Thaunat, A.-C. Field, J. Dai, L. Louedec, N. Patey, M.-F. Bloch, C. Mandet, M.-F. Belair, P. Bruneval, O. Meilhac, B. Bellon, E. Joly, J.-B. Michel, A. Nicoletti, Lymphoid neogenesis in chronic rejection: Evidence for a local humoral alloimmune response. *Proc. Natl. Acad. Sci.* **102**, 14723–14728 (2005).
61. A. Kratz, A. Campos-Neto, M. S. Hanson, N. H. Ruddle, Chronic inflammation caused by lymphotoxin is lymphoid neogenesis. *J. Exp. Med.* **183**, 1461–1472 (1996).
62. J. P. Stone, A. L. Ball, W. R. Critchley, T. Major, R. J. Edge, K. Amin, M. J. Clancy, J. E. Fildes, Ex vivo normothermic perfusion induces donor-derived leukocyte mobilization and removal prior to renal transplantation. *Kidney Int. Rep.* **1**, 230–239 (2016).
63. Y. Brewer, D. Taube, M. Bewick, G. Hale, F. Dische, A. Palmer, K. Welsh, C. Bindon, H. Waldmann, V. Parsons, S. Snowden, Effect of graft perfusion with two CD45 monoclonal antibodies on incidence of kidney allograft rejection. *The Lancet.* **334**, 935–937 (1989).
64. O. Thaunat, S. Graff-Dubois, N. Fabien, A. Duthey, V. Attuil-Audenis, A. Nicoletti, N. Patey, E. Morelon, A stepwise breakdown of B-cell tolerance occurs within renal allografts during chronic rejection. *Kidney Int.* **81**, 207–219 (2012).
65. T. S. Win, G. J. Pettigrew, Humoral autoimmunity and transplant vasculopathy: When allo is not enough. *Transplantation* **90**, 113–120 (2010).
66. G. Mieli-Vergani, D. Vergani, De novo autoimmune hepatitis after liver transplantation. *J. Hepatol.* **40**, 3–7 (2004).
67. D. Cosgrove, D. Gray, A. Dierich, J. Kaufman, M. Lemeur, C. Benoist, D. Mathis, Mice lacking MHC class II molecules. *Cell* **66**, 1051–1066 (1991).
68. Z. H. Chen, A technique of cervical heterotopic heart transplantation in mice. *Transplantation* **52**, 1099–1101 (1991).
69. G. C. Miescher, M. Schreyer, H. R. MacDonald, Production and characterization of a rat monoclonal antibody against the murine CD3 molecular complex. *Immunol. Lett.* **23**, 113–118 (1989).
70. D. P. Dialynas, Z. S. Quan, K. A. Wall, A. Pierres, J. Quintáns, M. R. Loken, M. Pierres, F. W. Fitch, Characterization of the murine T cell surface molecule, designated L3T4, identified by monoclonal antibody GK1.5: Similarity of L3T4 to the human Leu-3/T4 molecule. *J. Immunol.* **131**, 2445–2451 (1983).
71. J. Schindelin, I. Arganda-Carreras, E. Frise, V. Kaynig, M. Longair, T. Pietzsch, S. Preibisch, C. Rueden, S. Saalfeld, B. Schmid, J.-Y. Tinevez, D. J. White, V. Hartenstein, K. Eliceiri, P. Tomancak, A. Cardona, Fiji: An open-source platform for biological-image analysis. *Nat. Methods* **9**, 676–682 (2012).

Acknowledgments: We thank the staff of the flow cytometry platform (AniRA, SFR BioSciences, UMS34444/US8) and the staff of the animal facility (PBES, SFR BioSciences). We thank the NIH Tetramer Core Facility (Emory University) for providing tetramers. Servier Medical Art illustrations (under Creative Commons Attribution 3.0 Unported License) were used and modified to produce the figures (https://smart.servier.com/). **Funding:** The study was supported by funding from the Hospices Civils de Lyon (to X.C.), the Société Francophone de Transplantation (to X.C.), the Institut Hospitalo-Universitaire–Organ Protection and Replacement (IHU-OPeRa; ANR-10-IBHU-004 to C.-C.C.), the Agence Nationale pour la Recherche (ANR-12-PDOC-0019.01 and ANR-16-CE17-0007-01 to O.T.), the Fondation pour la Recherche Médicale (PME20180639518 to O.T.), and the Etablissement Français du Sang (to O.T.). **Author contributions:** X.C., C.-C.C., and O.T. conceived and designed the experiments. X.C., C.-C.C., S.H., D.G., C.S., M. Rabeyrin, M. Rabant, J.-P.D.v.H., A.K., V.M., L. Chalabreysse, S.G.-D., R.J.-M.,. A.T.-D., and J.-L.T. performed the experiments (X.C. performed cellular flow cross-match and single-antigen bead assay, mouse experiments, and analysis of perfusion liquids; X.C., S.G.-D., and R.J.-M. performed human cocultures; C.-C.C. performed heart transplantations, cellular flow cross-match, and mouse cocultures; S.H. performed $CD3^+$ chimerism in recipient's circulation; D.G. performed autoantibody test; C.S. and A.T.-D. performed collection and analysis of perfusion liquids; M. Rabeyrin, M. Rabant, J.-P.D.v.H., and L. Chalabreysse performed collection and analysis of mouse and human histopathological samples; A.K. performed imaging flow cytometry; V.M. and V.D. performed collection of HLA typing and anti-HLA immunization data; and J.-L.T. performed collection of HLA typing and anti-HLA immunization data and C1q assays). X.C., F.L., O.B., P.M., and J.I.P. acquired the clinical samples. X.C., C.-C.C., S.H., D.G., C.S., A.K., T.B., and O.T. analyzed the data. X.C. and O.T. wrote the original draft. J.-F.M., F.L., S.G.-D., P.M., L. Couzi, H.P., T.D., E.M., L.B., A.N., and V.D. revised the manuscript. **Competing interests:** O.T. participated in advisory boards for Biotest, Novartis, and AstraZeneca and received research grants from Immucor, bioMérieux, and BMS. The other authors declare that they have no competing interests. **Data and materials availability:** All data associated with this study are present in the paper or the Supplementary Materials.

Submitted 14 December 2020
Resubmitted 2 May 2022
Accepted 19 August 2022
Published 21 September 2022
10.1126/scitranslmed.abg1046

Science Translational Medicine

Inverted direct allorecognition triggers early donor-specific antibody responses after transplantation

Xavier Charmetant, Chien-Chia Chen, Sarah Hamada, David Goncalves, Carole Saison, Maud Rabeyrin, Marion Rabant, Jean-Paul Duong van Huyen, Alice Koenig, Virginie Mathias, Thomas Barba, Florence Lacaille, Jérôme le Pavec, Olivier Brugière, Jean-Luc Taupin, Lara Chalabreysse, Jean-François Mornex, Lionel Couzi, Stéphanie Graff-Dubois, Raphaël Jeger-Madiot, Alexy Tran-Dinh, Pierre Mordant, Helena Paidassi, Thierry Defrance, Emmanuel Morelon, Lionel Badet, Antonino Nicoletti, Valérie Dubois, and Olivier Thaunat

Sci. Transl. Med. **14** (663), eabg1046. DOI: 10.1126/scitranslmed.abg1046

Inverting immunity

A canonical pathway has been implicated in the development of donor-specific antibodies (DSAs) after transplantation. This pathway, called indirect allorecognition, occurs when a recipient's B cells target alloantigens on the graft, such as donor major histocompatibility complex (MHC) molecules. This is thought to rely on the recipient's CD4+ T cells providing help to the alloreactive B cells. However, Charmetant *et al.* found, using murine models, that development of DSAs can occur in the absence of recipient CD4+ T cells. Instead, donor-derived CD4+ T cells recognizing recipient MHC II molecules were capable of activating recipient B cells, a process the authors term "inverted direct allorecognition." The authors further showed that, in patients receiving allografts, transplant of tissues with higher passenger CD4+ T cell abundance correlated with early anti-MHC DSA responses, suggesting that this pathway is intact in humans as well.